Techno-economic evaluation and resource assessment of hydrogen production through offshore wind farms: a European perspective

Antoine Rogeau, Robin Girard, Matthieu de Coatpont, Julien Vieubled, Guillaume Erbs, Pedro H. Affonso Nobrega

Techno-economic evaluation and resource assessment of hydrogen production through offshore wind farms: a European perspective

Antoine Rogeau[a,b,*], Robin Girard[a,*], Matthieu de Coatpont[b], Julien Vieubled[b], Guillaume Erbs[b], Pedro Affonso Nobrega[a]

[a]*Mines Paris, PSL University, Centre for processes, renewable energy and energy systems (PERSEE), Sophia Antipolis, 06904, France*
[b]*ENGIE Impact, 1 place Samuel de Champlain, Courbevoie, 92400, France*

Abstract

Hydrogen demand is expected to radically increase in the upcoming years as it is a key lever of decarbonization and offshore wind has been identified as a credible energy source to power electrolyzers. Onshore, centralized offshore and decentralized offshore electrolysis are considered in this paper, for which a detailed cost modeling is carried out. A geospatial analysis leads to a resource assessment at European scale based on the levelized cost of hydrogen (LCOH), where both the energy production potential and technical and environmental constraints are considered.
The results reveal a massive resource in European seas, with LCOH decreasing from 4.5 - 7.5 €/kg in 2020 to 1.5 - 3.0 €/kg in 2050 due to the reduced costs of wind turbines and electrolyzers. A significant amount of green hydrogen - more than 1,000 TWh - could be produced at less than 3.0 €/kg in 2030 and 2.0 €/kg in 2050, making it competitive with grey hydrogen. In 2030, the mapping identifies a valuable 200 TWh resource where offshore wind-to-hydrogen projects offer a much-lower LCOH than their wind-to-power counterparts. The results of the resource assessment are detailed at country level, offering a valuable tool for energy modelers and local stakeholders. Finally, a detailed analysis of costs identifies offshore electrolysis as becoming more relevant over time: in 2020, offshore electrolysis is preferred for far-from-shore and deep-sea locations only while being located closer to shore in 2030 (over 100 km). In 2050, onshore electrolysis relevance is limited to locations close-to-shore in shallow waters.

Keywords: Hydrogen, wind power, wind-to-hydrogen, offshore, resource assessment, electrolysis, levelized cost of energy, geographical information system, cost modeling

Word count: 7881

Nomenclature

Acronyms

AHV	Anchor Handling Vessel
CAPEX	Capital Expenditure
COffE	Centralized Offshore Electrolysis
CTV	Crew-Transfer Vessel
DECEX	Decommissioning Expenditure
DOffE	Decentralized Offshore Electrolysis
EAR	Economically Attractive Resource
HLCV	Heavy-Lift Cargo Vessel
HVAC	High Voltage Alternative Current
HVDC	High Voltage Direct Current
JUV	Jack-Up Vessel

*Corresponding authors
Email addresses: antoine.rogeau@minesparis.psl.eu (Antoine Rogeau), robin.girard@minesparis.psl.eu (Robin Girard)

LCOH	Levelized Cost Of Hydrogen
OnE	Onshore Electrolysis
OPEX	Operational Expenditure
SOV	Service Offshore Vessel
SPIV	Self-Propelled Installation Vessel
SUBV	Self-Unloading Bulk Vessel
W2H	Wind-to-Hydrogen
W2P	Wind-to-Power

Subscripts and superscripts

BA	Base
C	Cable
CS	Connection slots
DS	Desalination system
EC	Export cable
EL	Electrolyzer
EP	Export pipeline
IA	Inter-array
IAP	Inter-array pipeline
$inst$	Installation
$load$	Loading
$loss$	Losses
maj	Major
MF	Manifold
$misc$	Miscellaneous
OP	Offshore platform
P	Pipeline
p	Pipe
PC	Power converter
PE	Platform equipment
PF	Platform foundation
PS	Power Substation
rep	Repair
s	Stage
SI	Sand island
TE	Turbine equipment
TF	Turbine foundation
$unload$	Unloading
WF	Wind farm
WT	Wind turbine

Variables

α	Multiplying factor	(-)
$\bar{V}_{H_2O}$	Nominal flow rate	(m^3/h)
$\dot{v}_{H_2O}$	Rated water consumption	(m^3/MWh)
η	Efficiency	(%)
λ	Failure rate	(f/year)
A	Area	(m^2)
BR	Bulk rate	(m^3/h)
C	Rated cost	(€/kW)
C_p	Capacitance	(F/km)
CD	Capacity density of wind farm	(MW/km^2)
d	Diameter of pipe	(m)
DP	Distance to port	(km)

DR	Day rate	(€/day)
E	Energy	(kg)
EC	Equipment cost	(€)
f	Frequency	(Hz)
h	Water depth	(m)
I	Intensity	(A)
IC	Installation cost	(€)
L	Length of element	(m)
l	Lifetime	(y)
LC	Linear cost	(€/m)
LIC	Linear installation cost	(€/m)
LoC	Logistics cost	(€)
MC	Maintenance cost	(€)
N	Number of elements	(-)
NL	Number of lifts	(h)
P	Power	(kW)
P^*	Equivalent electric power	(kW)
R	Resistance	(Ω)
r	Rate of return	(%)
S	Section of cable	(mm^2)
t	Time	(h)
U	Tension	(V)
UC	Unitary cost	(€)
V	Volume	(m^3)
VC	Vessel capacity	(units/lift)

1. Introduction

1.1. Context

The energy transition required to face the global environmental crisis can adopt various forms. While energy efficiency and sufficiency are both key levers to a cleaner future, the substitution of fossil fuels with cleaner alternatives has a major role to play. Electrification is often identified as the major decarbonization option, along with a reduction in the carbon content of the electricity mix. Nonetheless, some usages cannot be fully and directly electrified, mainly in industry (chemistry [1, 2], and steel production [3–5]), but also in heavy transport [6]. In such cases, hydrogen emerges as a credible option for decarbonization [6, 7].

Consequently, hydrogen demand - estimated at 339 TWh in 2019 in Europe [8] - is expected to drastically grow until 2050 and might reach up to 2,300 TWh in 2050 according to the European Hydrogen Backbone initiative [9], or even higher quantities depending on the scenario [10]. Today, hydrogen is mainly produced by steam methane reforming [11], a greenhouse gas emission-intensive process, and thus future hydrogen production must be widely decarbonized to represent a credible lever towards a carbon-free future. Water electrolysis is the main process identified as able to produce clean hydrogen at a large scale [11], as the electricity required for the process can be decarbonized (e.g. produced from renewable or nuclear sources). To foster the transition from grey/black to low-carbon hydrogen, the latter will need to be produced at a low cost.

One option being explored is the production of hydrogen from offshore wind, as shown by recent projects (Lhyfe [1], AquaVentus [2] or HT1 [3]). Indeed, dedicated offshore wind-to-hydrogen (W2H) is expected to enable far-from-shore wind development [12], involving fewer constraints on sea usage and the advantage of more constant, powerful winds. Moreover, wind turbine and electrolyzer costs are expected to decrease in the next years, thus promising a bright future for offshore wind projects.

[1] https://www.lhyfe.com/

[2] https://aquaventus.org/

[3] https://group.vattenfall.com/uk/what-we-do/our-projects/european-offshore-wind-deployment-centre/aberdeen-hydrogen

1.2. Background

Wind power has been widely investigated in the past as it is identified as a credible option to decarbonize power production. Hence, some detailed cost modelings have been published for wind-to-power (W2P) projects [13–16], often comparing HVAC and HVDC transport of power to shore. Depending on the level of detail, installation techniques [17] and costs are often considered [18–20], but also operation and maintenance [20–22] and decommissioning [20, 23, 24]. These modelings have sometimes been subject to specific adaptation, for example for floating structures in deep waters [25–28].
These cost-modeling approaches have been integrated into many resource assessment studies [29–31]. In particular, Martinez and Iglesias mapped the levelized cost of energy considering floating configurations in the European Atlantic [32] and Mediterranean Sea [33]. Beiter et al. [34] carried out a similar evaluation with a prospective focus in the United States. A site selection approach is also commonly developed aiming to identify areas compatible with wind projects [35–37]. The site selection and the economic assessment are sometimes coupled, for example by Caglayan et al. [38] and Hundleby and Freeman [39], the latter providing economically attractive resource curves at European scale.
Similar approaches have also been used for other ocean renewable energy, such as wave energy [40].

In contrast, hydrogen production from offshore wind farms is a relatively young field of research. Some works summarize the current situation of W2H [41–43], and identify three main connection schemes for such projects, namely onshore, centralized offshore, and decentralized offshore electrolysis. These connection schemes are also considered by Singlitico et al. [44] for an exemplar wind farm in the north sea, considering a parallel power-hydrogen export connection. Similarly, Lüth et al. [45] evaluate the most economical option between hydrogen and power connection for an energy island, considering grid infrastructure and capacity expansion. Lucas et al. [46] estimate the economics of hybridizing an existing wind-to-power project, analyzing the impact of electricity price variation on LCOH. Giampieri et al. [47] estimate the LCOH considering different energy carriers, such as hydrogen, power and ammonia, and the impact of hybridization on LCOH is analyzed for an exemplary wind farm.
Other works focus on the transport of energy, such as Miao et al. [48] and d'Amore Domenech et al. [49] who focus on the economic evaluation of pipeline, shipping, and power cable export options.
Some studies combine geographic analysis with economic evaluation for wind-to-hydrogen projects. For instance, Komorowska et al. [50] carry out a case-study in Poland, considering only onshore electrolysis. Dinh et al. [51] evaluate the LCOH of wind-to-hydrogen projects in Ireland, considering the centralized offshore connection scheme.
Finally, other studies are worth mentioning as they present similar analyses but for different ocean renewable energy: Serna and Tadeo [52] focus on wave energy while Babarit et al. [53] consider a dedicated fleet of energy ships.

1.3. Literature gaps and objective of the paper

In the view of the existing literature presented above, the following gaps are identified:

- The wind-to-hydrogen costs of floating offshore wind have not been properly modeled, especially for the decentralized connection scheme
- No harmonized comparison of onshore electrolysis has been made that considered HVAC and HVDC export and offshore electrolysis, and includes both centralized and decentralized options
- Few works combine the cost modeling with a prospective evolution of costs of wind turbines and electrolyzers
- A global resource assessment, similar to the ones published for wind-to-power, has not been conducted to date, yet it would enable the identification of the most economical sites and the overall potential of a study area

The objective of this work is thus to bring together the scattered cost models in the offshore wind and hydrogen production literature to develop a detailed cost modeling capable of considering the different connection schemes, for both onshore and offshore electrolysis. This cost modeling will then be integrated into a resource assessment at European scale. As the typologies of sites are very diverse in this wide study area, the cost modeling will be adapted to consider the impact of key on-site parameters, such as wind speed, water depth, distance to shore, and distance to port.

1.4. Methodology and paper outline

The levelized cost of hydrogen (LCOH) is adopted to evaluate and compare the profitability of hydrogen production from offshore wind farms. LCOH is derived from the lifetime costs and energy production over the lifetime of the project, as presented by Equation (1).

$$LCOH = \frac{\sum_{t=0}^{l} \frac{CAPEX_t + OPEX_t + DECEX_t}{(1+r)^t}}{\sum_{t=0}^{L} \frac{E_t}{(1+r)^t}} \tag{1}$$

where $CAPEX$, $OPEX$ and $DECEX$ are the capital, operational and decommissioning costs respectively (€), E is the produced energy or quantity of produced hydrogen (kg), l is the lifetime of the project (y), and r is the rate of return considered for the economic evaluation (%).

The required steps to perform the resource assessment are then threefold: (1) the total lifetime costs and (2) the energy production must be estimated at each location of the study area to estimate the LCOH, while (3) the suitable areas for offshore wind farm installation must be identified through a site selection procedure. The Economically Attractive Resource (EAR), defined as the quantity of energy that can be produced at a given price, can then be derived from the previous steps.

The global methodology is summarized in Figure 1.

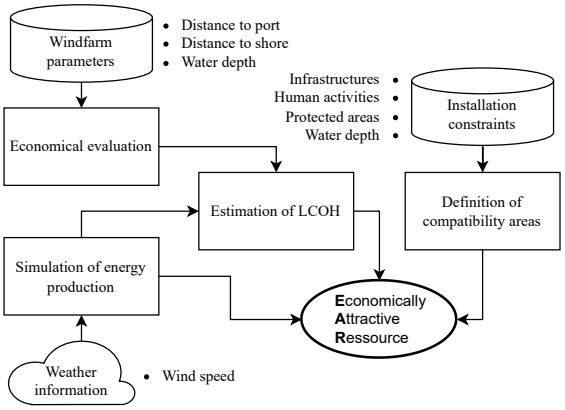

Figure 1: Flowchart of the developed methodology.

In accordance with the proposed methodology, the first section of this paper presents the connection schemes considered in this study before describing the detailed cost modeling adopted in the second section. The third section describes the estimation of the energy production of wind farms, and the fourth section presents the mapping procedure in detail. Finally, the overall methods are applied at European scale in the fifth section, which comprises a presentation and discussion of the results, such as the mapping of the LCOH, the drawing of economically attractive resource curves, and the detailed cost structures. A conclusion wraps up the key findings and draws out the main perspectives.

2. Connection schemes considered

Water electrolysis can be carried out onshore - power is transported to shore through power cables - or directly offshore and then transported to shore. In this paper, we consider pipeline transport of hydrogen although transportation by tankers can be advantageous for very long distances (over 1,000 km) [47–49].

We defined three connection schemes for hydrogen production, represented in Figure 2. The main elements involved in the conversion and transport chain of each configuration are presented in Table 1.

- **Scheme 1 - onshore electrolysis (OnE)**: The wind park can be connected to shore through an HVDC or HVAC power cable, depending on the distance [13–15]. In this case, hydrogen is produced by electrolyzers located onshore. This configuration has the advantage of requiring a small offshore platform (for power conversion

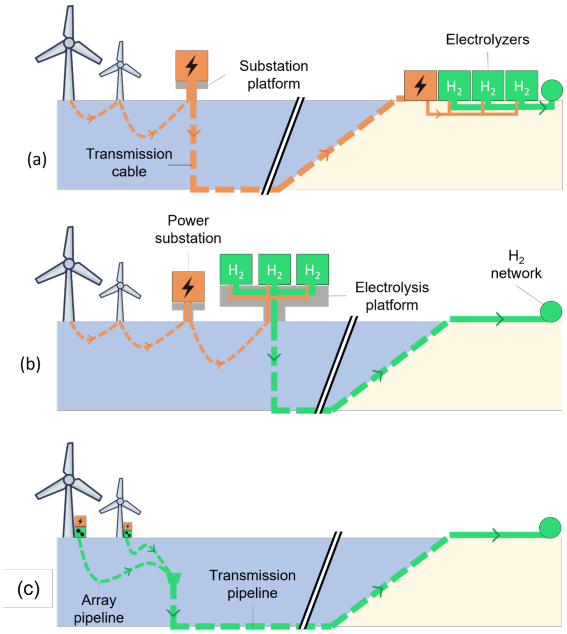

Figure 2: Different connection schemes considered: (a) Onshore electrolysis (b) Centralized offshore electrolysis (c) Decentralized offshore electrolysis.

systems only) but calls for expensive underwater array and transmission cables which also induce non-negligible power losses.

- **Scheme 2 - centralized offshore electrolysis (CoffE)**: Hydrogen can also be produced directly offshore. As electrolyzers are voluminous equipment, they require a dedicated platform. One option is to install the electrolyzers on a centralized platform at the wind farm. This configuration takes advantage of efficient, economic pipelines to transmit hydrogen to shore.
- **Scheme 3 - decentralized offshore electrolysis (DOffE)**: Another option for offshore production is to locate an electrolyzer close to each wind turbine. In this configuration, hydrogen is transported through individual inter-array pipelines to a manifold before being sent onshore through a rigid transmission pipeline. This configuration does not require building massive platforms and induces limited losses and costs.

This study estimates the cost of productin hydrogen on the coastline. Potential additional costs for connecting to transport infrastructures are considered as out of the scope of this paper.

3. Economical estimation of hydrogen production

In order to calculate the LCOH, we must first model the CAPEX, OPEX and DECEX. The CAPEX is composed of equipment costs, EC, and installation costs, IC, while the OPEX encompasses material costs, MC, and logistics costs, LoC.
The sizing of elements is very important in the calculation of equipment costs, and the losses at each step of the hydrogen production chain (see Sec. 4.2) are considered to adapt the sizing.

3.1. Equipment costs

3.1.1. Wind turbines

The cost of wind turbines can be split between two elements, namely the turbine foundation (TF) and the turbine equipment (TE).

Table 1: Elements of the transmission chain for the different connection schemes as defined in Fig. 2. n is the number of wind turbines.

			Offshore	
		Onshore	Centralized	Decentralized
Power substation	HVDC/HVAC offshore substation	X		
	HVDC onshore substation	X		
	Power converter		X	n.X
Hydrogen production	Electrolyzers	X	X	n.X
	Desalinator		X	n.X
	Electrolysis platform		X	
Transmission	Array cables	X	X	
	Array pipelines			X
	Transmission cables	X		
	Transmission pipeline		X	X

$$EC_{WT} = EC_{TE} + EC_{TF} \tag{2}$$

Fixed-bottom and floating wind turbines are considered, with the turbine costs being common to both configurations [54]. Both the turbine and foundation costs are directly related to the number of turbines N_{WT} and their rated power P_{WT} (kW) through a rated cost RC (€/kW) as presented in Equations (3) and (4).

$$EC_{TE} = N_{WT} \cdot RC_{TE} \cdot P_{WT} \tag{3}$$

$$EC_{TF} = N_{WT} \cdot RC_{TF}(h) \cdot P_{WT} \tag{4}$$

The rated cost of turbines is expected to decrease over the years, while the rated power of wind turbines is expected to evolve oppositely, thus reducing the number of wind turbines per wind farm, and consequently the investment, installation and operation costs. Corresponding hypotheses are presented in Table 2.

Table 2: Evolution of wind turbine costs and technical parameters. Sources: [54, 55]

	2020	2030	2050	
RC_{TE}	1,500	1,200	1,000	(€/kW)
Rated power	8	15	20	(MW)

Regarding the foundations, three options are considered:

- Monopile for shallow water, i.e. less than 25 meters deep
- Jacket for depths between 25 and 55 meters
- Floating for waters deeper than 55 meters

The modeling of rated cost of foundations is based on Bosch et al. [54], and is dependent on water depth, h (m), as presented in Equation (5).

$$RC_{TF}(h) = c_1 \cdot h^2 + c_2 \cdot h + c_3 \cdot 10^3 \tag{5}$$

The coefficients c_1, c_2 and c_3 differ with the foundation type and decrease with time, as presented in Table 3. The coefficient values of Bosch et al. [54] are adjusted to match the projections of RTE [55]. Depending on the water

depth and the installation year, the foundation costs will represent between 16% and 60% of the total wind turbine costs.

Table 3: Evolution of coefficients used for the foundation costs of wind turbines (see Eq. 5) Sources: Estimations based on [54] and [55]

		Turbine foundation		
		Monopile	Jacket	Floating
2020	c_1	201	114	0
	c_2	613	- 2,270	774
	c_3	812	932	1,481
2030	c_1	181	103	0
	c_2	552	- 2,043	697
	c_3	370	478	1,223
2050	c_1	171	97	0
	c_2	521	- 1,930	658
	c_3	170	272	844

In the case of decentralized offshore electrolysis, the foundation of the wind turbines must be adapted to accommodate the electrolyzers (e.g. by adding a dedicated platform). As the foundation costs are driven by the weight to support, this modification is modeled through an additional cost fixed at 20% of the foundation cost because the power density of the electrolyzers is estimated as 20% of the power density of the wind turbine (based on manufacturers' data and our own estimations).

3.1.2. Offshore platforms

Offshore electrolyzers and power substations require a dedicated platform. The cost of offshore platforms is modeled similarly as for wind turbines (see Sec. 3.1.1), and incorporates the cost of platform equipment (PE) and platform foundations (PF).

$$EC_{OP} = EC_{PE} + EC_{PF} \tag{6}$$

EC_{PE} depends on the installed equipment and is defined further on in this article (see Sec. 3.1.3 for power substations and Sec. 3.1.4 for electrolysis plants).

Three types of platform can be constructed to host the equipment, depending on the water depth at the location:

- Sand islands are used in shallow waters (depth under 30 meters), as they significantly reduce investment costs when the size of the wind farm increases. For this reason, they are planned for energy hubs in the North Sea [44]
- Jacket platforms are considered for deeper waters, up to 150 meters
- For deep seas (depth over 150 meters), floating platforms are required

.

3.1.2.1 Sand island

The cost of a sand island EC_{SI}, presented in Equation (7), depends on the volume of sand V_{SI} (m^3) and the area to protect A_{SI} (m^2), which are defined by Singlitico et al. [44]. Substation and electrolyzer footprints of 5 m^2/MW and 20 m^2/MW are considered respectively [44, 56].

$$EC_{SI} = C_{SI,V} \cdot V_{SI}(h) + C_{SI,A} \cdot A_{SI}(h) \tag{7}$$

Table 4: Cost parameters of sand islands. Source: [44]

$C_{SI,V}$	3.26	(€/m^3)
$C_{SI,A}$	804.00	(€/m^2)

Table 5: Evolution of coefficients used for the foundation costs of platforms. Sources: Estimations based on [57, 58]

		Platform foundation	
		Jacket	Floating
RC	c_2	233	87
	c_3	47	68
UC	c_2	309	116
	c_3	62	91

3.1.2.2 Jacket and floating platforms

The modeling of the foundation costs - presented in Equation (8) - is inspired by the cost modeling of turbine foundations (see Eq. (4)). The dependence on water depth is simplified to a piecewise linear function, and calibrated to match literature values [32, 44, 57, 58]. The coefficients employed to estimate the rated cost and the unitary cost of the foundations (RC_{PF} and UC_{PF}) are presented in Table 5.

$$EC_{PF} = RC_{PF}(h) \cdot P^*_{WF} + UC_{PF}(h) \tag{8}$$

Due to the novelty of dedicated electrolysis platforms, no cost data or modelings are available in the literature and thus the identified cost data mainly concern platforms hosting power substations. Consequently, the foundation cost is expressed as a function of equivalent electric power P^*_{WF}. Based on manufacturers' data and our own assumptions, HVDC substations are considered to have twice the power density (in W/kg) of electrolyzers and half the power density of HVAC platforms [14, 32], and so P^*_{WF} is calculated by Equation (9).

$$P^*_{WF} = \begin{cases} P_{WF} & \text{if HVDC substation,} \\ 0.5 \cdot P_{WF} & \text{if HVAC substation,} \\ 2 \cdot P_{WF} & \text{if electrolysis plant.} \end{cases} \tag{9}$$

3.1.3. Power substation

The equipment costs of power substation EC_{PS} vary with the wind farm capacity and the type of substation (HVAC or HVDC), as presented in Equation (10).

$$EC_{PS} = RC_{PS} \cdot P_{WF} + UC_{PS} \cdot 10^3 \tag{10}$$

Power substation cost hypotheses are presented in Table 6.

Table 6: Cost parameters of HVDC and HVAC substations. Source: [14, 44, 59, 60]

	HVDC	HVAC	
RC_{PS}	102.93	22.87	(€/kW)
UC_{PS}	31.75	7.06	(M€)

3.1.4. Electrolysis plant

3.1.4.1 Electrolyzers

The cost of electrolyzers is expected to radically decrease by 2050, thus increasing the affordability of green hydrogen [11]. Proton exchange membrane electrolyzers are the preferred option for offshore production, due to their higher pressure output, limited footprint and operating temperature [44, 61]. The equipment cost EC_{EL} is modeled by Equation (11), considering a scaling effect and a learning rate [62].

$$EC_{EL} = RC_{EL} \cdot P_{EL} \tag{11}$$

where

$$RC_{EL} = \left(k_0 + k \cdot p_{EL}^{\alpha-1}\right) \cdot \left(\frac{Y}{Y_0}\right)^{\beta} + RC_0 \tag{12}$$

where k_0 and k are constants, P_{EL} is the electrolyzer rated power (kW_e), and Y and Y_0 are the installation year and reference year, respectively. RC_0 is an additional fixed cost representing the electrolyzer-to-system cost (connection, sealing, etc.), decreasing over time, which is considered to match the literature values [56, 60]. This cost doubles when the electrolyzer is located offshore [44].

Figure 3 represents the evolution of electrolyzer-rated costs with the rated power of equipment, for the years 2020, 2030, and after 2040 considering the parameter values presented in Table 7.

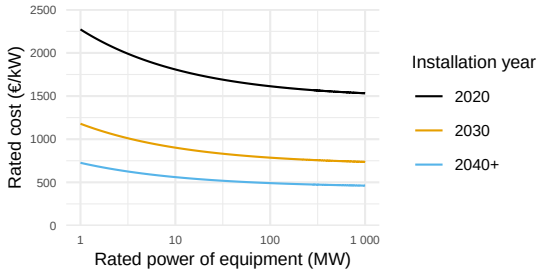

Figure 3: Evolution of electrolyzer-rated costs with time. Source: adapted from [62]

Table 7: Cost parameters of electrolysis systems. Source: [62]

k_0	673.73	(€)
k	10,876.93	(€)
α	0.662	-
Y_0	2020	-
β	-104.45	-

The maximum rated power of electrolyzers is expected to increase in the coming years. In 2022, a maximum rated power of 20 MW is considered, reaching 200 MW by 2050. When needed, multiple electrolyzers are installed to correspond to the total wind farm power.

3.1.4.2 Power converter

For offshore production schemes, as wind turbines provide an AC current while electrolyzers require a DC current, power converters and circuit breakers are required and the cost of power conversion EC_{PC} (€) is estimated by Equation (13). The corresponding cost hypotheses are presented in Table 8 [60].

$$EC_{PC} = RC_{PC} \cdot P_{PC} \tag{13}$$

3.1.4.3 Desalinator

Offshore hydrogen production requires desalination of seawater to produce the large quantity of freshwater needed for electrolysis. The cost of desalination system EC_{DS} is estimated by Equation (14) [44].

$$CAPEX_{DS} = RC_{DS} \cdot \bar{V}_{H_2O} \tag{14}$$

where RC_{DS} is the rated cost of the desalinator (€/(m^3/h)) and $\bar{V}_{H_2O}$ is the nominal flow rate of water (m^3/h).

The desalinator is sized at 80% of the rated power of electrolyzers P_{EL} (kW), considering a small buffer storage of freshwater. The nominal flow rate of water is then related to the nominal power of the electrolyzer by Equation (15), where the rated water consumption of electrolyzers $\dot{v}_{H_2O}$ is estimated at 0.263 m^3/MWh [63].

$$\bar{V}_{H_2O} = \dot{v}_{H_2O} \cdot 0.8 \cdot P_{EL} \tag{15}$$

Table 8: Cost parameters of conversion elements. Source: [44, 64]

RC_{PC}	104.13	(€/kW)
RC_{DS}	30.56	(€/m^3)
$\dot{v}_{H_2O}$	263	(m^3/kW)

3.1.5. Inter-array connection

3.1.5.1 Electric inter-array connection

Except for decentralized offshore configuration, the power produced by the wind turbines is transmitted to a substation through inter-array cables. The investment cost of inter-array cables EC_{IA} depends on the length and section of the cables. A string-based layout, represented in Figure 4, is considered, and the section of cables S increases along the array, within the limit of its capacity. The total inter-array cost is estimated by Equation (16).

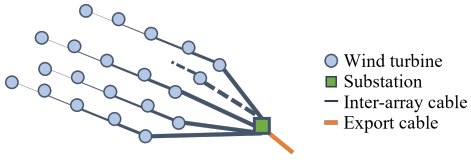

Figure 4: Schematic string-based layout considered for wind farms in onshore and centralized offshore electrolysis configurations. The electrolyzers are located on the platform or onshore.

$$EC_{IA} = N_A \cdot \left(\sum_i LC_{S_i} \cdot L_{S_i} + LC_{S_{max}} \cdot L_{S_{max},HUB} \right) \tag{16}$$

where N_A is the number of required arrays, and LC_{S_i} and L_{S_i} are the linear cost (€/m) and the total length (m) of inter-array cables of section S_i respectively. S_{max} is the largest cable section required and $L_{S_{max},HUB}$ is the length of cable required to connect the arrays to a sand island hub if needed (see Sec. 3.1.2.1).

The techno-economical parameters of inter-array cables are presented in Table 9. Both 66kV and 132kV cables are considered as the rating tension increases with the rated power of turbines.

The length of cable of section S_i is calculated as described in Equation (17). The number of wind turbines connected on this section N_{S_i} depends on the remaining available capacity, considering the wind turbines connected to the upstream sections. We limit to 8 the number of turbines per array in order to limit power losses.

Table 9: Technico-economical assumptions for inter-array cables. Sources: [59, 65–68] and own assumptions.

i	Tension (kV)	Section (mm^2)	Resistance (Ω/km)	Capacity (MW)	Cost dynamic (€/m)	Cost static (€/m)	Inst. cost (€/m)
1	66	95	0.25	24	180	113	113
2		150	0.16	30	215	134	121
3		300	0.08	42	298	186	149
4		400	0.06	49	357	223	156
5		630	0.04	59	456	285	171
6		800	0.03	69	577	361	180
1	132	120	0.2	80	288	152	114
2		150	0.16	87	358	188	122
3		300	0.08	123	747	393	216
4		400	0.06	136	900	474	213
5		630	0.04	162	1228	646	226
6		800	0.03	201	1779	936	281

$$L_{S_i} = N_{S_i} \cdot L_{IA} \tag{17}$$
$$\text{with } N_{S_i} = \lfloor \frac{P_{S_i} - \sum_{k=1}^{i-1} N_{S_k} \cdot P_{WT}}{P_{WT}} \rfloor$$

where L_{IA} is the length of the inter-array cable between two turbines (m) and is estimated as presented by Equation (18) [69]. The mean distance between two turbines $D_{WT} = \sqrt{\frac{P_{WT}}{CD_{WF}}}$ depends on CD_{WF} and P_{WT}, the capacity density (MW/km^2) and the rated power (MW) of the wind turbines respectively.

$$L_{IA} = 2 \cdot 2.6 \cdot h + D_{WT} \tag{18}$$

When the water depth exceeds 200 m, laying the inter-array cables on the seabed is not economical and they as thus suspended [70, 71]. To ensure the continuity of LCOH at this frontier, the failure rate (see Sec. 4.3) of suspended cables is considered as 10% greater than for laid cables.

When connected to a sand island, the length of the static cable needed is estimated considering the formula presented in [44]. Otherwise, the arrays are connected to a centralized platform and the additional cable length $L_{S_{max},HUB}$ is equal to D_{WT}.

3.1.5.2 Pipeline inter-array connection

In the case of decentralized production (i.e. an electrolyzer in each turbine), hydrogen is collected by flexible pipes which are connected to the transport pipeline by manifolds, as represented in Figure 5. Manifolds have a limited number of connection slots N_{CS} which implies that manifolds are cascaded in N_s connection stages, calculated by Equation (19).

$$N_s = \left\lceil log_{N_{CS}}(N_{WT}) \right\rceil \tag{19}$$

At each stage i, the length of pipes needed is estimated by Equation (20), which depends on the number of pipes N_p connected to each of the $N_{MF,i}$ manifolds in this stage i and on A_i which is the total area covered by the

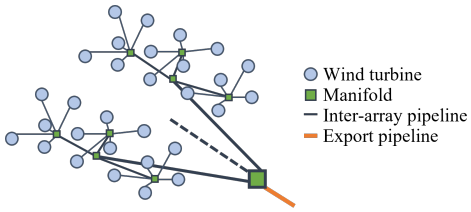

Figure 5: Schematic radial layout considered for wind farms in a decentralized offshore electrolysis configuration. An electrolyzer is located in each wind turbine.

downstream wind turbines (km^2). The first pipe stage (from the turbines to the seabed) comprises flexible pipes, while the remaining stages use rigid pipes.

$$L_i = \begin{cases} N_{WT} \cdot \left(\frac{\sqrt{A_i}}{\sqrt{2}} + h\right), & \text{if } i = 1 \\ N_p \cdot N_{MF,i} \cdot \frac{\sqrt{A_i}}{\sqrt{2}}, & \text{otherwise} \end{cases} \tag{20}$$

Inter-array pipeline equipment costs (EC_{IAP}) are then calculated by Equation (21).

$$EC_{IAP} = \sum_{i=1}^{N_s} \left(\alpha_s(d_i) \cdot LC_{BA,IAP} + LC_{misc,IAP}(d_i)\right) \cdot L_i \tag{21}$$

where $\alpha_s(d)$ and $LC_{misc}(d)$ are a size factor and a miscellaneous cost (for more details and values, see [72]) and LC_{BA} is the base cost of flexible pipes (€/m), defined in Table 10.

The diameter of the pipeline at stage i (d_i (m)) is estimated recursively, based on the diameter of the export pipeline (see Eq. (29)), as defined in Equation (22). A minimum diameter of 5 cm is considered.

$$d_i = \max\left(0.05, \frac{d_{i-1}}{\sqrt{N_c}}\right) \tag{22}$$

Manifolds are used to connect pipes in groups, and then to the transmission pipeline. The cost model is similar to inter-array pipelines, as it depends on the diameter of the connected pipelines. In this work, we consider that each manifold has 5 connection slots, except for the final manifold which can have less slots. The total cost of manifolds EC_{MF} is expressed by Equation (23).

$$EC_{MF} = \sum_{i=1}^{N_s} \Big(\alpha_s(d_i) \cdot \alpha_N(N_{CS}) \cdot UC_{BA,MF} + UC_{misc,MF}\Big) \cdot N_{MF,i} \tag{23}$$

where $\alpha_s(d)$ and $\alpha_N(N_{CS})$ are factors depending on the pipeline diameter and the number of connection slots respectively. For more details and values, see [72]. UC_{BA} and UC_{misc} are the base and miscellaneous costs respectively (€), defined in Table 10.

3.1.6. Energy export

As a conservative assumption, the total length L of the export cable or pipeline is considered as 1.2 times the distance to shore DS_{WF}.

Table 10: Main parameters values used for pipes (flexible and rigid) and manifold costs estimation. Source: [72]

N_{CS}		5	(slots)
LC_{BA}	Flexible	1736.73	(€/m)
	Rigid	173.67	(€/m)
UC_{BA}	Manifold	2.265	(M€)
$UC_{misc,MF}$		0.188	(M€)

Table 11: Techno-economical assumptions for HVAC export cables. Sources: [13, 65–68] and own assumptions

Tension (kV)	Section (mm^2)	Resistance (mΩ/km)	Capacitance (nF/km)	Ampacity (A)	Cost (€/m)	Inst. Cost (€/m)
132	630	39.5	209	818	406	335
	800	32.4	217	888	560	340
	1000	27.5	238	949	727	350
220	500	48.9	136	732	362	350
	630	39.1	151	808	503	360
	800	31.9	163	879	691	370
	1000	27.0	177	942	920	380
400	800	31.4	130	870	860	540
	1000	26.5	140	932	995	555
	1200	22.1	170	986	1130	570
	1400	18.9	180	1015	1265	580
	1600	16.6	190	1036	1400	600
	2000	13.2	200	1078	1535	615

$$L = 1.2 \cdot DS_{WF} \tag{24}$$

For the onshore electrolysis scheme, an export cable is needed. Both HVAC and HVDC export cables are considered, as the most economical solution can vary, mainly depending on the distance to shore, the breakeven point being located at a transport distance of around 50-80 km [13–15]. For the offshore electrolysis scheme, an export pipeline is considered.

3.1.6.1 HVDC cable

The investment cost of the HVDC export cable $EC_{EC,HVDC}$ is described by Equation (25).

$$CAPEX_{EC,HVDC} = RC_{EC,HVDC} \cdot P_{EC,HVDC} \cdot L_{EC} \tag{25}$$

where $RC_{EC,HVDC}$ is the linear cost of the cable, estimated at 1.35 €/W/km [16, 67], $P_{EC,HVDC}$ is the rated power of the export cable (MW) and L_{EC} is the length of the export cable.

3.1.6.2 HVAC cable

The power capacity of HVAC cables decreases non-linearly with distance, so that as the distance to shore increases, the section of HVAC cables must be reduced and several cables must be installed in parallel [13].

The cables considered in this study are presented in Table 11.

The power capacity of the cable P_{EC} (W) is estimated by Equation (26) [13] and the adequate cable section and rated tension are selected to minimize the number of cables $N_{EC,HVAC}$ and consequently costs.

$$P_{EC} = \sqrt{(\sqrt{3} \cdot U \cdot I)^2 - (\frac{1}{2} \cdot U^2 \cdot 2\pi \cdot f \cdot C_p \cdot L_{EC})^2} \tag{26}$$

where U is the cable voltage (V), I is the ampacity of the line (A), f is the frequency, considered to be 50 Hz, and C_p is the capacitance (F/km).

The investment cost of the HVAC export cables $EC_{EC,HVAC}$ is then calculated by Equation (27).

$$EC_{EC,HVAC} = N_{EC,HVAC} \cdot LC_{EC,HVAC} \cdot L_{EC} \tag{27}$$

where $LC_{EC,HVAC}$ is the linear cost of cable (€/m), presented in Table 11.

3.1.6.3 Rigid pipeline

If the electrolyzers are located offshore, the hydrogen produced must be transmitted to shore through an export pipeline. The same cost modeling is adopted for the export pipeline as for inter-array pipes (see Sec. 3.1.5.2) as presented in Equation (28).

$$EC_{EP} = \Big(\alpha_s(d) \cdot LC_{BA,EP} + LC_{misc,EP}(d)\Big) \cdot L_{EP} \tag{28}$$

As for inter-array pipes, cost coefficients are presented in Table 10, and rigid pipes are considered for export.

The diameter of the export pipeline increases with the distance to shore and the power of the wind power plant, as more hydrogen has to flow through the pipeline and the pressure drop is significant [42]. Equation (29) models the evolution of the export pipeline diameter d_{EP} (m).

$$d_{EP} = 0.200 + 0.346 \cdot 10^{-3} \cdot L_{EP} + 0.065 \cdot P_{EP} \cdot 10^{-9} \tag{29}$$

where L_{EP} is the length of the pipeline (m).

3.2. Installation costs

3.2.1. Wind turbines

A simplified version of the modeling developed by Kaiser and Snyder [18] is used in this paper. Installation costs depend on:

- the characteristics of the vessel needed to transport the turbines (speed, capacity and daily rate).
- the time and equipment needed to install the turbines on site.

The generic installation cost of wind turbines IC_{WT} (€) is calculated as presented in Equation (30).

$$IC_{WT} = \left(NL \cdot \left(\frac{2 \cdot DP_{WF}}{v} + t_{load}\right) + t_{inst} \cdot N_{WT}\right) \cdot \frac{DR}{24} \tag{30}$$

where $NL = \frac{N_{WT}}{VC_b}$ is the number of lifts required, VC_b is the vessel capacity (units/lift), DP_{WF} the distance to the closest port (km), v is the speed of the vessel (km/h), t_{load} the loading time of each lift (h), t_{inst} the installation times of the wind turbine (h), and DR is the dayrate of the vessel (€/d).

Fixed wind turbines are transported using a Self-Propelled Installation Vessel (SPIV) which ensures both the transport and the assembly of turbines and foundations. The number of turbines transported per lift depends on their rated power, and vessel capacity is fixed at 40 MW/lift. The number of lifts needs to be doubled as the foundations also need to be transported and installed.

Floating wind turbines are assembled onshore and then towed to the farm's location using tugboats where they are moored by specialized vessels called Anchor Handling Vessels (AHV). Three tugboats are required to transport a floating wind turbine while a single AHV can moor 7 of them.

Table 12 summarizes the input parameters.

Table 12: Parameters of the vessels used for wind turbine installation. *: Depends on the rated power of turbines. Sources: [17, 18, 25, 27, 73, 74]

			Floating		
		Fixed	Trans.	Ancho.	
Vessel		SPIV	Tug	AHV	
Capacity	VC	*	0.3	7	(u/lift)
Speed	v	18.5	7.5	18.5	(km/h)
Load. time	t_{load}	24	5	30	(h/lift)
Inst. time	t_{inst}	144	-	90	(h/u)
Dayrate	DR	200	2.5	40	(k€/d)

Table 13: Parameters of the vessels used for platform installation. Sources: [18, 27]

			Floating		
		Fixed	Trans.	Ancho.	
Vessel		SPIV	HLCV	AHV	
Capacity	VC	1	1	3	(u/lift)
Speed	v	18.5	22.5	18.5	(km/h)
Load. time	t_{load}	24	10	30	(h/lift)
Inst. time	t_{inst}	96	-	90	(h/u)
Dayrate	DR	200	40	40	(k€/d)

3.2.2. Platforms

Fixed platforms are installed using SPIVs, just like fixed wind turbines. Floating substations require Heavy-Lift Cargo Vessels (HLCV). The input parameters are provided in Table 13.

For the installation of sand islands, the sand has to be loaded, transported and unloaded at the farm's location using Self-Unloading Bulk Vessels (SUBV). The sand island installation costs IC_{SI} are estimated by Equation (31) and the input parameters are summarized in Table 14.

$$IC_{SI} = \left(\frac{V_{SI}}{VC_{SUBV}} \cdot \frac{2 \cdot DP_{WF}}{v_{SUBV}} + \frac{V_{SI}}{BR_{load}} + \frac{V_{SI}}{BR_{unload}} \right) \cdot \frac{DR}{24} \tag{31}$$

Table 14: Parameters of the vessels used for sand island construction. Source: own assumptions

		Sand island	
Vessel		SUBV	
Capacity	VC	20,000	(m^3/lift)
Speed	v	25	(km/h)
Load. rate	BR_{load}	2,000	(m^3/h)
Unload. rate	BR_{unload}	6,000	(m^3/h)
Dayrate	DR	15	(k€/d)

3.2.3. Cables and pipes

The installation costs of cables are modeled through a linear cost representing laying and burying expenditures [67], as presented by Equation (32).

$$IC_C = LIC_C \cdot L_C \tag{32}$$

where LIC is the linear installation cost of the cable (€/m), which considers the laying and burying cost, and L_C is the length of the cable to be installed (m). The values of the installation costs of inter-array cables and HVAC export cables are presented in Tables 9 and 11 respectively. For HVDC export cables, an installation cost of 50% of the equipment cost is considered [67].

The installation costs of pipes are modeled by considering that Flex-lay or S-lay vessels are required for infield and export pipelines respectively. The installation costs of pipes IC_{CP} are calculated as presented by Equation (33) and the corresponding inputs are presented in Table 15.

$$IC_P = \frac{L_{EP}}{LR} \cdot DR \tag{33}$$

Table 15: Parameters of the vessels used for pipeline installation. Sources: adapted from [75–78]

		Pipeline		
		IA	Exp.	
Vessel		Flex	S-Lay	
Lay. rate	LR	7.0	4.0	(km/d)
Dayrate	DR	400	700	(k€/d)

3.3. OPEX

Operation and maintenance costs primarily depend on the need for replacement spare parts but also increase with the distance to port, as ships need to reach the wind farm.

Operation and maintenance costs are defined by two elements: the material cost MC (€) which consists in replacing equipment parts, and the logistics costs LoC (€). Additionally, energy losses in conversion and transport can be assimilated to operation costs.

3.3.1. Repair costs

The repair costs of the different elements of the hydrogen production chain, defined as a percentage of the equipment costs, are presented in Table 16.

Table 16: OPEX values of power chain elements, defined as a share of the equipment costs (*Onshore/offshore values). Sources: [44, 60, 79]

	MC (% EC)
Wind turbines	2.5%
Sand island	1.5%
HVDC/HVAC substation	1.5%/3%*
Electrolyzers	2%/4%*
Power converters	1%/2%*
Desalinator	3%
Power cables	0.2%
Pipelines	2%

3.3.2. Logistics costs

The logistics costs correspond to the cost of reaching the turbines for maintenance with specialized vessels.

Minor repairs are carried out using light vessels. An onshore-based strategy, using Crew Transfer Vessels (CTV) can be adopted when the farm is close to shore. A mothership-based strategy, using Service Offshore Vessels (SOV),

is more suitable for large or far-from-shore farms, avoiding very long-distance travel and increasing the availability of turbines [22, 80–82].

The considered maintenance strategy aims to guarantee a wind farm availability of 94%, as observed in many existing cases [83, 84]. The logistics costs are modeled as linearly increasing up to 150 km from shore, where an SOV strategy stabilizes the costs, as presented in Figure 6.

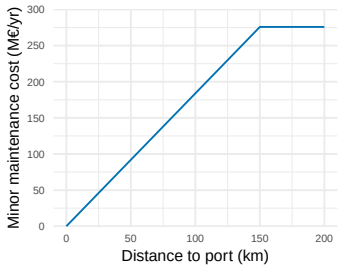

Figure 6: Evolution of minor maintenance costs of wind turbines and conversion equipment. Source: adapted from [80, 82, 85]

Major repairs require more significant interventions, and the maintenance of fixed wind turbines is realized *in-situ* with a Jack-Up Vessel (JUV), while floating wind turbines need to be towed to port or to an assembly area in order to be repaired [21].

The yearly logistics costs for major repairs LoC_{maj} are calculated using Equation (34), the corresponding parameters being presented in Table 17

$$LoC_{maj} = N_{WT} \cdot \lambda_{maj} \cdot \left(\frac{2n \cdot DP_{WF}}{v} + t_{rep}\right) \cdot \frac{DR}{24} \tag{34}$$

where λ_{maj} is the failure rate, considered as 0.08 failures per year [80], and n is the number of roundtrips required for major maintenance.

Table 17: Parameters of the vessels used for major wind turbine repairs. Sources: [21, 80]

		Fixed	Floating	
Vessel		JUV	Tug	-
Speed	v	18.5	7.5	(km/h)
Repair time	t_{rep}	50	50	(h)
Dayrate	DR	150	2.5	(k€/d)
Roundtrips	n	1	2	-

3.4. DECEX

Decommissioning operations are very similar to installation processes. For the sake of simplification, the decommissioning cost structure is considered as being the same as for installation, but the removal times are significantly lower. The considered times for decommissioning elements are presented in Table 18. For inter-array and export cables, a decommissioning cost of half the installation cost is considered.

4. Energy production

4.1. Wind power production

Power production is derived from wind speed through the theoretical wind farm power curves presented in Figure 7. The power curves evolve over time, due to the tendency of increasing the swept area of wind turbines to produce power at lower wind speeds [86].

Table 18: Decommissioning times or removal rates. Sources: [24]

	Decom. time /Removal rate	
Fixed turbine	144	(h)
Anchors	30	(h)
Fixed platform	96	(h)
Export pipeline	5	(km/d)
IA pipeline	10	(km/d)

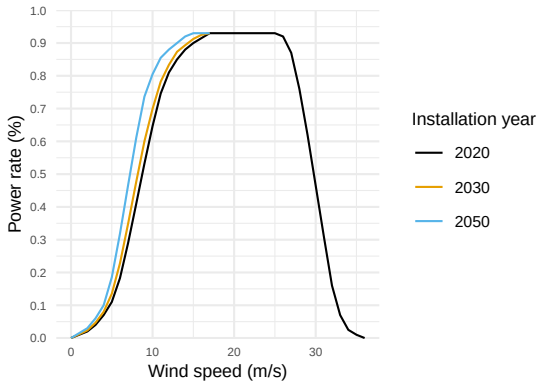

Figure 7: Wind farm power curves considered for the different installation years. Sources: [86]

4.2. Energy losses

Energy losses occur at each step of the hydrogen production chain and reduce the final energy production. These losses can occur during transmission (see Tab. 19) or conversion (see Tab. 20). The specific energy consumption of a desalination plant is about 4 kWh/m^3 [64], representing about 0.1% of the electrolyzer consumption. Losses in the HVAC cables (IA and export) are estimated along the whole year and are detailed in Equation (35) [65].

Table 19: Loss values along the hydrogen transmission chain. Sources: [47, 60, 87]

	Losses	
Array cables	**	(%)
Array pipes	0.03	(%/1000)
Export cables	3.0	(%/1000)
Export pipelines	0.03	(%/1000)

$$\eta_{HVAC} = 1 - \sum_t \frac{P_{loss}(t)}{P_{prod}(t)} \tag{35}$$
$$\text{with } P_{loss} = \left(\frac{P_{prod}(t)}{U}\right)^2 \cdot R \cdot L$$

where $P_{prod}(t)$ is the power flowing through the cable at moment t, and R is the linear resistance as defined in Table 9. Losses are calculated section by section along the array cables, and along the export cable.

4.3. Failure rates and unavailability of the wind farm

When a failure occurs anywhere in the production, conversion or transmissions steps, a share of the production is lost due to the unavailability of part or all of the wind farm. As presented in Section 3.3.2, the maintenance costs are

Table 20: Efficiency values along the hydrogen production chain. Sources: [11, 47, 56, 60, 87]

		Efficiency
HVDC substation		99 %
Power converters		99.5 %
Electrolyzers	2020	62 %
	2030	65 %
	2050	70.5 %
Desalinator		99.9 %

modeled to guarantee a global availability of wind turbines and electrolyzers of 94%.

Power cables and pipelines can also be subject to failures, leading to complete or partial unavailability of the production; and the longer the connection, the higher the failure rate. The considered failure rates and repair times are presented in Table 21.

Table 21: Failure rates and repair times considered for cables and pipelines. *: repair time for inter-array and export cable respectively. Sources: [88, 89]

		Failure rate (f/yr/km)	Repair time (d)
Cable	HVAC	0.003	40/60*
	HVDC	0.0015	60
Pipeline	Flexible	0.001	40
	Rigid	0.0001	60

5. Mapping of the resource

The economic modeling presented above aims to estimate the European economically attractive resource of hydrogen produced from offshore wind. To do so, a site selection must be carried out before estimating the site-specific costs of hydrogen production schemes at each location.

5.1. Site selection

The site selection problem has been widely investigated in the past in both the academic literature [35, 36]and technical reports [39]. Thus, the methodology developed in this work for identifying suitable zones for WP development will not be presented in detail.

Following the methodology of Hundleby and Freeman [39], we consider four restriction levels - with four associated wind farm densities:

- General: No particular restriction, maximum wind farm coverage is set at 56% to leave space for ships' movement and wake effect
- Sensitive: Minor restrictions, reducing the maximum coverage by 20%, and setting it to 45%
- Very sensitive: Major restrictions implying sparser wind farms. The maximum coverage is reduced by 50%, and set at 28%
- Exclusion: wind farms cannot be constructed

The considered constraints are detailed in Table 22, along with the defined thresholds. Two new custom constraints are considered, and derived from global datasets. Maritime routes are deducted from EMODnet data [90] where routes are considered dense (medium respectively) when more than 1000 routes per square meter per year are observed (500 resp.). Fishing effort data are provided by the Global Fishing Watch based on AIS data [93]. The considered threshold for exclusion (resp. Very sensitive and Sensitive) corresponds to the 5% most fished waters (resp. 10% and 20%).

Table 22: Constraints considered for the identification of suitable zones and thresholds defined for the four restriction levels. Sources: [37, 39]

			Exclusion	Very sensitive	Sensitive	General	Data
Distance	Maritime routes (m)	Dense	< 3,500			> 3,500	[90]
		Medium	< 1,500			> 1,500	[90]
	Power cables (m)		< 500		< 1,500	> 1,500	[90]
	Telecom. cables (m)		< 500		< 1,500	> 1,500	[90]
	Existing wind farms (km)		< 8			> 8	[90]
	Shore (km)		< 10		< 20	>20	[91]
Value	Depth (m)		> 1000				[92]
	Fishing effort (h/km^2/yr)		> 24.6	> 14.5	> 6.7	< 6.7	[93]
	Wind power density (W/m^2)		< 500				[94]
Exclusion zones	Human activities		Aggregate extr.				[90]
			Munitions				[90]
	Protected areas		IUCN Ia - III	IUCN IV - VI			[95]
				Natura 2000			[95]
				RAMSAR			[95]

5.2. LCOH estimation at European scale

To estimate the LCOH at European scale, the following four inputs are provided as geographical information:

- Distance to shore: the shoreline, ignoring small islands, is used to calculate the shortest distance to shore
- Distance to ports: ports of size M and L from the World Port Index [96] are considered as suitable for offshore activities. Distance to port is calculated using a grid distance avoiding land
- Depth: bathymetry information from EMODnet is used [92]
- Wind speed: Eleven years (2010-2020) of ERA-5 hourly wind speed at 100m [94] are used for the analysis, as this database is reliable for offshore wind assessment [97]

For this study, the installed capacity of wind farms is set at 1GW with a capacity density of 6 MW/km^2, in accordance with observed values [98, 99]. Finally, a lifetime of 25 years and a rate of return of 5% are considered. The resolution of all datasets is set at 5km x 5km, to be compatible with the large perimeter of the resource assessment.

6. Results and discussion

6.1. Resource assessment

6.1.1. Mapping of the resource

The lifecycle costs, the LCOH, and the energy potential are estimated for the whole European maritime space. Results of the evaluation are visualized as maps in Figure 8, which represent yearly energy and LCOH over Europe in 2030. Iceland is excluded from the scope of the evaluation, as it is unlikely to participate in a European hydrogen market.

Figure 8 (a) provides a visual representation of the constraints on wind projects. About 43% of European seas are unavailable due to depth over 1000 m, 34% are excluded due to technical or environmental constraints as defined in Section 5.1, and about 7% are subject to non-exclusive constraints. The latter are characterized by a reduced yearly energy production, in grey on the map.

The North Sea and waters close to the United Kingdom and Ireland are identified as areas where large quantities of hydrogen can be produced at low LCOH on Figure 8 (b). On the contrary, the Mediterranean Sea only offers a limited resources of expensive hydrogen.

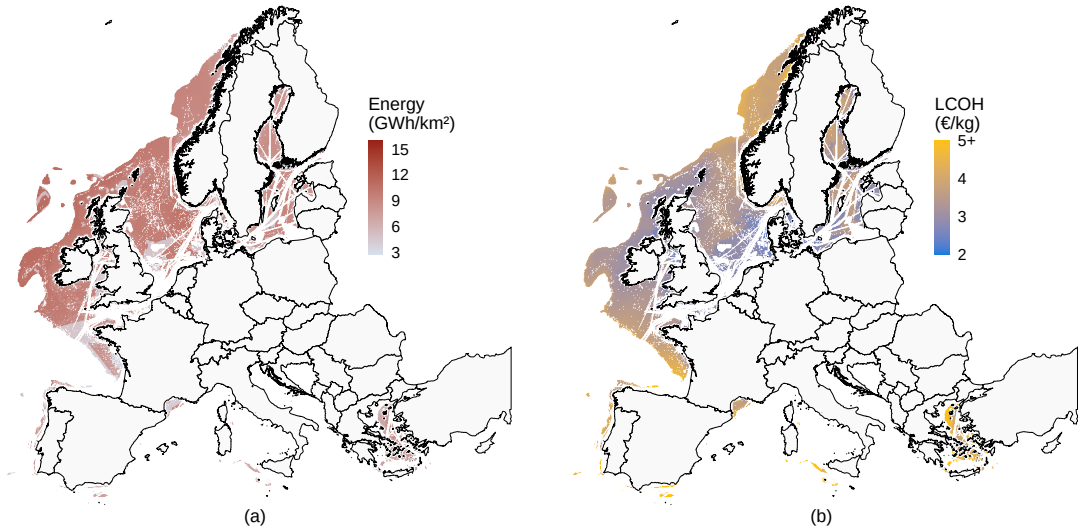

Figure 8: European maps of European (a) yearly energy production and (b) LCOH in 2030.

6.1.2. Economically attractive resource

The European potential can be visualized as a merit order, ranked by LCOH. These curves are drawn from 2020 to 2050, shown in Figure 9. The potential grows over time - from about 10,000 TWh/yr in 2020 to 13,750 TWh/yr in 2050 - due to the increase of both the efficiency of electrolyzers and the swept area of turbines. These potentials are massive compared to the hydrogen consumption in Europe in 2020 (339 TWh [8]) and expected in 2050 (664 to 4,000 TWh [10]). In the theoretical case where all European hydrogen is produced by wind-to-hydrogen projects, the most expensive hydrogen would range from 1.5 €/kg to 5.5 €/kg depending on the installation year.

The curves also pan to the left, representing the reduction of LCOH in Europe over time. In 2020, 1,250 TWh can be produced yearly at a cost of under 5.0 €/kg, while all of the 13,750 TWh available in European seas can be produced at less than 3.5 €/kg in 2050. The cheapest hydrogen can be produced at 4.5 €/kg in 2020 and decreases to 1.5 €/kg by 2050.

In 2020, the production cost of grey hydrogen (e.g. from methane cracking) was estimated at 2 €/kg, making wind-to-hydrogen projects competitive by 2050. This cost recently exploded due to the high natural gas price, reaching about 6 €/kg, and could also increase with a higher carbon tax, thus making wind-to-hydrogen projects even more competitive, or bringing them forward.

6.1.2.1 Sensitivity analysis

Since wind turbine and electrolyzer costs hypothesis are critical for the economic evaluation, a sensitivity analysis is carried out, considering the following variations:

- The cost of wind turbines, especially floating, is hard to predict. Uncertainty margins of ± 400 €/kW in 2030 and ± 600 €/kW in 2050 are considered, based on values projected by [55].
- The evolution of the cost of electrolyzers is very uncertain [100]. Alternative higher and lower electrolyzer costs are considered by reducing the β coefficient, which represents the learning curve effect over the years, from -100 to -50 for the higher case and to -150 for the lower case. A 100 MW electrolyzer will thus cost 935 €/kW in 2030 and 800 €/kW in 2050 for the higher case (670 €/kW and 470 €/kW for the lower case).

Figure 9 represents the evolution of the EAR curves as a confidence interval, in 2030 and 2050. The minimum hydrogen cost range is 2.25 - 2.9 €/kg in 2030, with a 1,250 TWh/yr potential at less than 2.6 - 3.3 €/kg. In 2050, the cost range drops to 1.2 - 1.9 €/kg and a 1,250 TWh/yr potential below 1.3 - 2.2 €/kg. This variation, which is

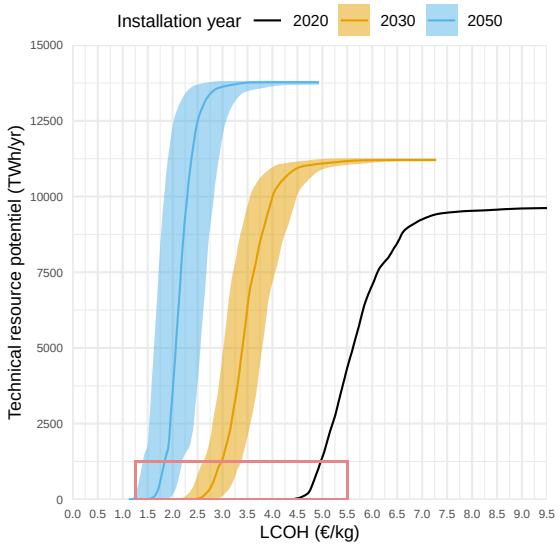

Figure 9: Evolution of the economic resource with installation years. Shaded area: resource range sensitized to electrolyzer and wind turbine costs. Rectangle: focus area of Fig. 10.

constant along the EAR curve as it does not depend on depth and distance to shore, is about ± 0.3 €/kg in 2030 and ± 0.4 €/kg in 2050.

6.1.2.2 Competing usages of offshore wind and pertinence of offshore electrolysis

In the frame of the European Green Deal, offshore wind installed capacity is expected to grow by 450 GW by 2050 [101]. As a first analysis, and even though this power production will be partly dedicated to hydrogen production, we consider that this sea usage competes with dedicated offshore hydrogen production.

The two facets on Figure 10 represent the evolution of the low-cost resource (part of the EAR curve highlighted on Fig. 9), depending on whether we consider that the most economical sites identified for Onshore Electrolysis might be dedicated to wind-to-power. The same plot features both the original resource curve, which considers wind-to-hydrogen, and an additional resource curve that represents the economic resource if onshore electrolysis is the only option considered. This analysis highlights the interest of considering offshore electrolysis schemes and leads to the following conclusions:

- By considering the competing usage of offshore wind, the LCOH of the cheapest hydrogen is increased by about 18%, whatever the year of installation
- Offshore electrolysis has almost no impact on the low-cost resource in 2020 as this solution is not competitive, but does substantially reduce the LCOH from 2030 onwards, whether or not some spots are reserved for W2P
- The savings made thanks to offshore production schemes increase with the LCOH, as the most expensive resource is located far from shore and/or in deep waters, where the offshore production schemes are the most advantageous
- The most economical sites for the 450 GW of W2P do not totally overlap with the best sites for W2H. A resource of about 200 TWh is accessible at a much lower LCOH (-10%) when considering offshore production schemes. In 2050, the cost advantage of W2H schemes is observable all along the low-cost resource curve

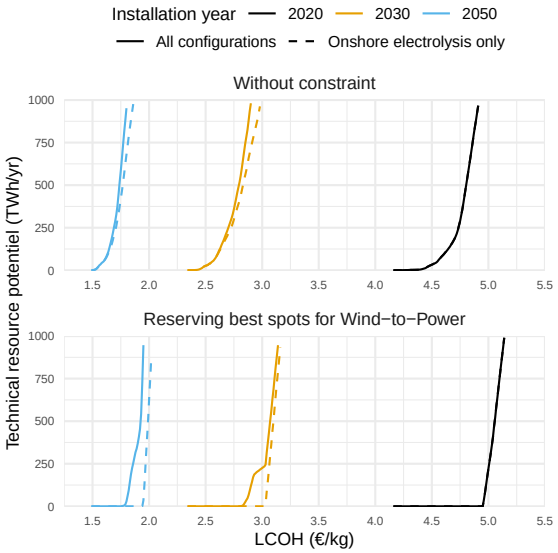

Figure 10: Evolution of the resource at low LCOH when considering offshore or onshore electrolysis only. Upper plot: all sites are available for hydrogen production; Lower plot: 450 GW of capacity is reserved for Wind-to-Power.

6.1.3. By-country potential estimation

The European map of LCOH can also be used to conduct country-level analyses using Exclusive Economic Zones (EEZ).

The EAR curves for nine European countries are presented in Figure 11, with a particular emphasis on the most economical connection scheme.

This focus highlights the wide diversity of contexts, as some countries can be identified as providers of low-cost hydrogen, such as Denmark, Germany and the Netherlands, where centralized offshore hydrogen production overtakes the potential, but present limited total resources while others, such as France, Norway and Sweden, have large potential but at a higher cost. Note that for some extreme northern countries such as Norway, part of the seas might be hard to exploit due to ice coverage, and their resource is thus overestimated. Ireland and the United Kingdom both present significant potential with reasonable LCOH, making them key stakeholders in future hydrogen production from offshore wind.

This data is of great interest for the energy modeling community and local stakeholders seeking the best location for wind-to-hydrogen projects. For this reason, several datasets are provided for further usage and openly available [102], namely:

- The mapping of the LCOH for each connection scheme, the final LCOH, the preferred option and the energy production. When relevant, sensitized costs hypotheses and evolution with years are included
- The Economically Attractive Resource curves at European and national scales, including Iceland
- Visualization of the above-mentioned datasets

.

Even though Iceland have been excluded from the scope of the study, its maps and EAR curves are provided as supplementary material.

6.2. Comparison of connection schemes

Figure 12 represents the preferred connection scheme to produce hydrogen from offshore wind. This map highlights that onshore electrolysis is limited to close-to-shore locations, due to the high costs and energy losses from power cables. HVAC is preferred for close-to-shore locations. A limited area - mainly in the North Sea - is dedicated

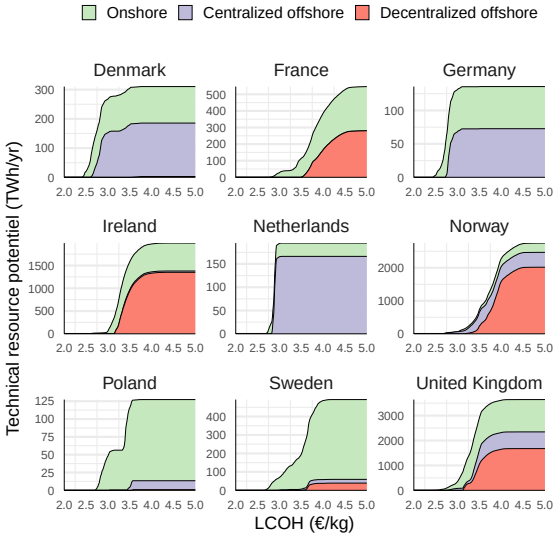

Figure 11: National economically attractive resource curves in 2030, declined by type of connection scheme. Caution: Y axis differs from one country to another.

to centralized offshore electrolysis due to the limited costs of platforms in shallow waters. Finally, decentralized offshore hydrogen production is the preferred option for far-from-shore and deep locations.

6.2.1. Cost structure analysis

Six sites, represented in Fig. 12, are selected to cover the variety of typologies in terms of water depth and distance to shore (and port). The characteristics of the selected sites are presented in Table 23.

Table 23: Characteristics of the sites selected for in-depth cost structure comparison (see location of points on Fig. 8).

	Distance				
ID	Shore (km)	Port (km)	Depth (m)	lon (°)	lat (°)
A	39.2	205.2	13	14.73	54.36
B	66.0	159.6	126	4.08	42.85
C	45.0	203.8	960	-8.94	43.76
D	248.3	309.2	27	3.51	55.18
E	184.7	253.8	134	-7.83	49.17
F	291.2	437.1	796	-14.30	50.98

The lifetime cost structure and the LCOH for the six sites are presented in Figure 13.

The offshore electrolysis connection schemes offer much lower transmission costs as pipelines are less expensive than power cables. Nonetheless, an additional platform or wind turbine adaptation costs are required for the centralized and decentralized offshore connection schemes respectively. The cost of a platform is high in deep-sea waters for the centralized options while the inter-array costs are non-negligible for the decentralized alternative, as flexible pipes need to be laid on the seabed. In the end, onshore electrolysis is almost always the most economical option in terms of pure total lifetime costs, followed by centralized offshore and decentralized offshore options, in that order.

The LCOH does not behave strictly the same way as total lifetime costs, as energy losses and unavailability of the wind farm are considered. Onshore electrolysis is the most economical option to produce hydrogen close to shore, even though the observed differences are smaller for LCOH than for total costs, and the decentralized offshore scheme is almost competitive in very deep waters. In contrast, the offshore electrolysis options are by far the more

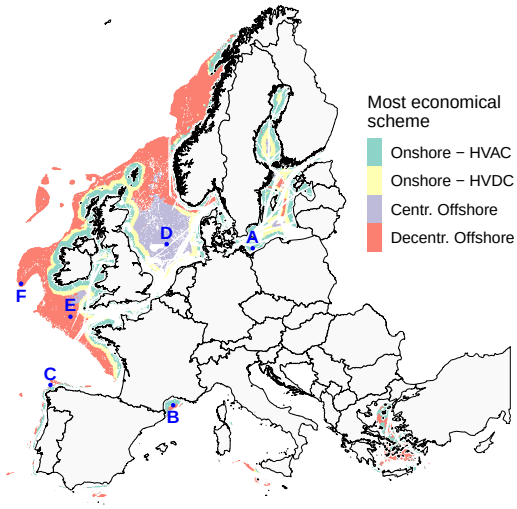

Figure 12: European map of most economical schemes in 2030. Red points: study cases for cost comparison (see Sec. 6.2.1).

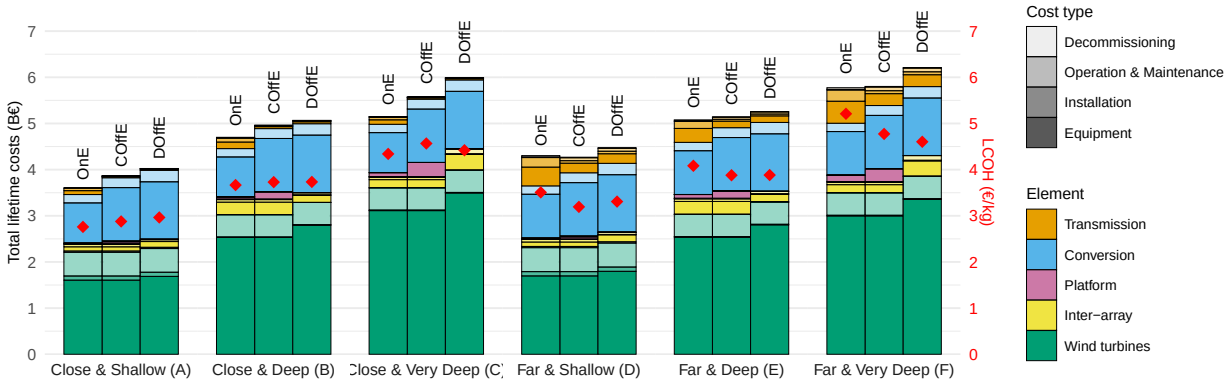

Figure 13: Lifetime costs structure and LCOH for the six selected sites in 2030.

economical when considering far-from-shore locations, the centralized option being preferred for shallow waters and the decentralized option for deep sea. This inversion is due to the low losses in pipelines and their lower failure rate.

6.2.2. Evolution of break-even points

Due to the evolution of electrolyzer costs, the points where one scheme becomes more economical than another evolve over the years. Figure 14 represents the evolution of the LCOH offered by each connection scheme with the installation year. In 2020, the centralized option is preferred almost everywhere, except for far and very deep locations. As seen earlier, the onshore configuration remains the most economical close to shore in 2030 but is however less competitive than offshore electrolysis. In 2050, the offshore connection schemes are preferred in almost every situation except for close-to-shore and shallow waters.

To emphasize these observation, Figure 15 shows the most commonly observed connection schemes depending on the distance to shore and depth of location, based on the evaluation at European scale.

The following observation can be made:

- The break-even point between onshore and offshore hydrogen production in shallow waters (up to 100 m) decreases over time. In 2020, it is more economical to produce hydrogen from power transported to shore

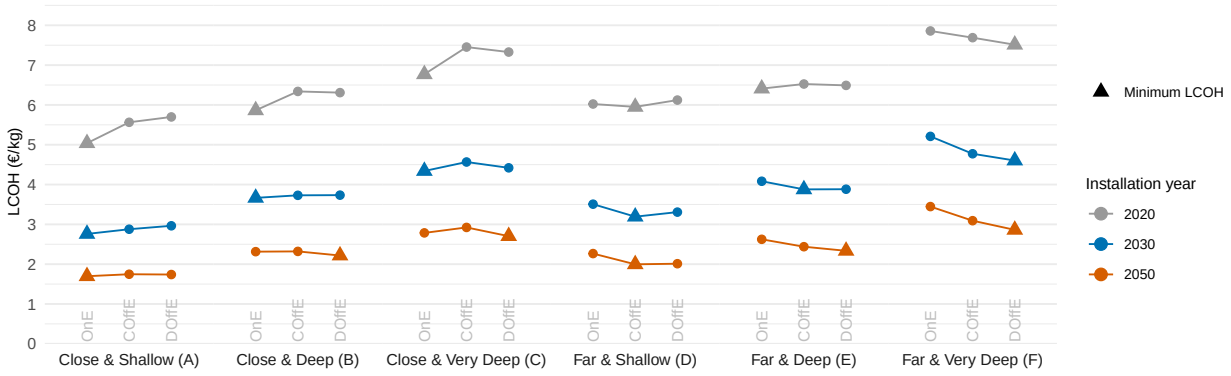

Figure 14: Evolution of the LCOH with year of installation.

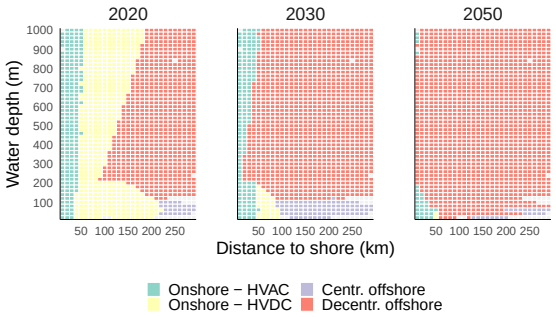

Figure 15: Most observed connection scheme in European seas depending on the distance to shore and water depth.

through power cables than to produce it up to 200 km offshore, while the break-even point is located around 80 km in 2030 and decreases to 50 km in 2050. This is mainly due to the high reduction of electrolyzer costs, which means that the additional cost of installing the electrolyzer offshore is balanced by the lower cost of pipeline transportation and increased availability

- Decentralized offshore hydrogen production is preferred to a centralized scheme in deep waters (over 100 m) when the platform costs and the inter-array losses become prohibitive. In 2050, the decentralized option is even preferred in shallow waters as the scaling effect of installing small electrolyzers is reduced (see Sec. 3.1.4.1)
- From 200 m and as water depth increases, onshore electrolysis becomes more economical than offshore schemes. Indeed, inter-array pipelines are laid on the seabed while suspended inter-array cables are more economical
- The break-even point between HVAC and HVDC connections is located around 50 km, which is in line with the literature

As a final observation, one can argue that even when offshore electrolysis is more economical, the construction of wind farms dedicated to hydrogen production prevents the power being used for other purposes. Indeed, the missed opportunity of selling power when electricity prices are high, and of producing hydrogen when they are low could change the equilibrium and extend the zone of relevance of onshore hydrogen production. Nonetheless, for far-from-shore locations, offshore electrolysis is by far more economical than its onshore counterpart and should be considered. This analysis is supported by Figure 14, where the LCOH differences at locations close to shore are very small.

The mapping of preferred option is also provided as supplementary material, and openly available [102].

7. Conclusions and future work

Low-carbon hydrogen production is a key lever for the decarbonization of hard-to-tackle emitting sectors. Consequently, this work presents a detailed bottom-up economic evaluation of offshore wind-to-hydrogen projects, which is used to carry out a resource assessment at European scale. The results provide evidence that offshore production of hydrogen, coupled with transportation through a pipeline, can be economical in many configurations, and gain competitiveness over the years, making it a credible option from 2030. The global mapping produced using geographical information systems enables an evaluation at country-scale and is of interest for the energy modeling community and local stakeholders. The reduced costs of wind-to-hydrogen production thanks to offshore electrolysis configuration are also visualized considering future competing wind-for-power developments.

Despite the contribution of this work, some future research should be carried out to deepen the analysis.
First, transportation by tanker could be included in the analysis for very far and/or very deep sites, thus requiring a proper optimization of hydrogen storage. The produced hydrogen could be transported liquefied, as such, or as ammonia.
Secondly, this analysis does not consider the cost of missed opportunity of producing electricity, as dedicated wind farms are considered. The optimization of hydrogen/power production for the onshore electrolysis configuration and the consideration of an additional export cable or a fuel cell for offshore configurations could make the resource even more economical. Similarly, it could be insightful to evaluate hybrid wind-and-solar configuration to further increase the load factor of electrolyzers and reduce the corresponding LCOH.
The adjusted production costs of hydrogen in waters with a frequent ice coverage, such as in Norway, could also be investigated to identify new opportunities.
Finally, the LCOH has been estimated at shore, and the potential cost of connection to existing infrastructure is not considered. Consequently, LCOH estimated in remote areas such as North Sweden might be significantly underestimated. On the contrary, existing infrastructures, such as decommissioned oil and gas platforms and pipelines, could be repurposed and used for hydrogen production [103–106].
All these points could be the object of further studies.

Acknowledgments

This work results from a partnership between Mines Paris - PSL, ENGIE Impact France and ENGIE SA, in the frame of the program "France Relance / Préservation de l'Emploi R&D" partially funded by the French Ministry of Higher Education and Scientific Research.

Data availability

Datasets related to this article can be found at `https://doi.org/10.5281/zenodo.8036703`, an open-source online data repository hosted at Zenodo [102]. The following information is provided:

- Datasets resulting from the modeling as maps in NetCDF format, including maps of LCOH for each connection scheme, final LCOH, energy production and preferred option.
- Visualization of the above datasets in the form of national maps
- Dataset of EAR curves at European and national scale, sensitized as in 6.1.2.1
- Visualisation of the above sensitized EAR curves

Disclaimer

The present paper does not reflect the vision of ENGIE Group but only the ideas of the authors.

References

[1] L. Mosca, E. Palo, M. Colozzi, G. Iaquaniello, A. Salladini, S. Taraschi, Hydrogen in chemical and petrochemical industry, in: Current Trends and Future Developments on (Bio-) Membranes, Elsevier, 2020, pp. 387–410. doi:10.1016/B978-0-12-817384-8.00017-0.

[2] F. Kullmann, J. Linßen, D. Stolten, The role of hydrogen for the defossilization of the German chemical industry, International Journal of Hydrogen Energy (2023). doi:10.1016/j.ijhydene.2023.04.191.

[3] W. Choi, S. Kang, Greenhouse gas reduction and economic cost of technologies using green hydrogen in the steel industry, Journal of Environmental Management 335 (2023) 117569. doi:10.1016/j.jenvman.2023.117569.

[4] M. Shahabuddin, G. Brooks, M. A. Rhamdhani, Decarbonisation and hydrogen integration of steel industries: Recent development, challenges and technoeconomic analysis, Journal of Cleaner Production 395 (2023) 136391. doi:10.1016/j.jclepro.2023.136391.

[5] P. Marocco, M. Gandiglio, D. Audisio, M. Santarelli, Assessment of the role of hydrogen to produce high-temperature heat in the steel industry, Journal of Cleaner Production 388 (2023) 135969. doi:10.1016/j.jclepro.2023.135969.

[6] S. van Renssen, The hydrogen solution?, Nature Climate Change 10 (2020) 799–801. doi:10.1038/s41558-020-0891-0.

[7] Michael Liebreich/Liebreich Associates, Clean Hydrogen Ladder, Version 4.1, 2021.

[8] J. Cihlar, A. Villar Lejarreta, A. Wang, F. Melgar, J. Jens, P. Rio, Hydrogen generation in Europe: Overview of costs and key benefits, Technical Report, European Commission, 2021. doi:10.2833/821682.

[9] A. Wang, J. Jens, D. Mavins, M. Moultak, M. Schimmel, K. Van der Leun, D. Peters, M. Buseman, Analysing future demand, supply, and transport of hydrogen, Technical Report, European Hydrogen Backbone Initiative, 2021.

[10] H. Blanco, W. Nijs, J. Ruf, A. Faaij, Potential for hydrogen and Power-to-Liquid in a low-carbon EU energy system using cost optimization, Applied Energy 232 (2018) 617–639. doi:10.1016/j.apenergy.2018.09.216.

[11] IEA, The Future of Hydrogen - Seizing today's opportunities, Technical Report, International Energy Agency, 2019. URL: https://www.capenergies.fr/wp-content/uploads/2019/07/the_future_of_hydrogen.pdf.

[12] R. Peters, J. Vaessen, R. v. d. Meer, Offshore Hydrogen Production in the North Sea Enables Far Offshore Wind Development, in: Day 4 Thu, May 07, 2020, OTC, 2020. doi:10.4043/30698-MS.

[13] X. Xiang, M. Merlin, T. Green, Cost Analysis and Comparison of HVAC, LFAC and HVDC for Offshore Wind Power Connection, in: 12th IET International Conference on AC and DC Power Transmission (ACDC 2016), Institution of Engineering and Technology, 2016, pp. 6 (6 .)–6 (6 .). doi:10.1049/cp.2016.0386.

[14] B. Van Eeckhout, D. Van Hertem, M. Reza, K. Srivastava, R. Belmans, Economic comparison of VSC HVDC and HVAC as transmission system for a 300 MW offshore wind farm, European Transactions on Electrical Power (2009). doi:10.1002/etep.359.

[15] L. P. Lazaridis, Economic Comparison of HVAC and HVDC Solutions for Large Offshore Wind Farms under Special Consideration of Reliability, Ph.D. thesis, Royal Institute of Technology, Stockholm, 2005. URL: https://www.diva-portal.org/smash/get/diva2:609080/FULLTEXT01.pdf.

[16] S. Lauria, M. Schembari, F. Palone, M. Maccioni, Very long distance connection of gigawatt-size offshore wind farms: extra high-voltage AC versus high-voltage DC cost comparison, IET Renewable Power Generation 10 (2016) 713–720. doi:10.1049/iet-rpg.2015.0348.

[17] Z. Jiang, Installation of offshore wind turbines: A technical review, Renewable and Sustainable Energy Reviews 139 (2021) 110576. doi:10.1016/j.rser.2020.110576.

[18] M. J. Kaiser, B. F. Snyder, Modeling offshore wind installation costs on the U.S. Outer Continental Shelf, Renewable Energy 50 (2013) 676–691. doi:10.1016/j.renene.2012.07.042.

[19] D. Ahn, S.-c. Shin, S.-y. Kim, H. Kharoufi, H.-c. Kim, Comparative evaluation of different offshore wind turbine installation vessels for Korean west–south wind farm, International Journal of Naval Architecture and Ocean Engineering 9 (2017) 45–54. doi:10.1016/j.ijnaoe.2016.07.004.

[20] R. Chitteth Ramachandran, C. Desmond, F. Judge, J.-J. Serraris, J. Murphy, Floating offshore wind turbines: installation, operation, maintenance and decommissioning challenges and opportunities, Wind Energy Science Discussions (2021).

[21] J. McMorland, M. Collu, D. McMillan, J. Carroll, Operation and maintenance for floating wind turbines: A review, Renewable and Sustainable Energy Reviews 163 (2022) 112499. doi:10.1016/j.rser.2022.112499.

[22] Z. Ren, A. S. Verma, Y. Li, J. J. Teuwen, Z. Jiang, Offshore wind turbine operations and maintenance: A state-of-the-art review, Renewable and Sustainable Energy Reviews 144 (2021) 110886. doi:10.1016/j.rser.2021.110886.

[23] C. Milne, S. Jalili, A. Maheri, Decommissioning cost modelling for offshore wind farms: A bottom-up approach, Sustainable Energy Technologies and Assessments 48 (2021) 101628. doi:10.1016/j.seta.2021.101628.

[24] M. J. Kaiser, B. Snyder, Modeling the decommissioning cost of offshore wind development on the U.S. Outer Continental Shelf, Marine Policy 36 (2012) 153–164. doi:10.1016/j.marpol.2011.04.008.

[25] J. Altuzarra, A. Herrera, O. Matías, J. Urbano, C. Romero, S. Wang, C. Guedes Soares, Mooring System Transport and Installation Logistics for a Floating Offshore Wind Farm in Lannion, France, Journal of Marine Science and Engineering 10 (2022) 1354. doi:10.3390/jmse10101354.

[26] K. Saeed, J. McMorland, M. Collu, A. Coraddu, J. Carroll, D. McMillan, Adaptations of Offshore Wind Operation and Maintenance Models for Floating Wind, Journal of Physics: Conference Series 2362 (2022) 012036. doi:10.1088/1742-6596/2362/1/012036.

[27] L. Castro-Santos, A. Filgueira-Vizoso, I. Lamas-Galdo, L. Carral-Couce, Methodology to calculate the installation costs of offshore wind farms located in deep waters, Journal of Cleaner Production 170 (2018) 1124–1135. doi:10.1016/j.jclepro.2017.09.219.

[28] C. Maienza, A. M. Avossa, F. Ricciardelli, F. Scherillo, C. T. Georgakis, A Comparative Analysis of Construction Costs of Onshore and Shallow- and Deep-Water Offshore Wind Farms, 2019, pp. 440–453. doi:10.1007/978-3-030-12815-9{_}35.

[29] P. Elsner, Continental-scale assessment of the African offshore wind energy potential: Spatial analysis of an under-appreciated renewable energy resource, Renewable and Sustainable Energy Reviews 104 (2019) 394–407. doi:10.1016/j.rser.2019.01.034.

[30] R. P. Patel, G. Nagababu, S. S. Kachhwaha, V. A. K. Surisetty, A revised offshore wind resource assessment and site selection along the Indian coast using ERA5 near-hub-height wind products, Ocean Engineering 254 (2022) 111341. doi:10.1016/j.oceaneng.2022.111341.

[31] J. P. Arenas-López, M. Badaoui, Analysis of the offshore wind resource and its economic assessment in two zones of Mexico, Sustainable Energy Technologies and Assessments 52 (2022) 101997. doi:10.1016/j.seta.2022.101997.
[32] A. Martinez, G. Iglesias, Mapping of the levelised cost of energy for floating offshore wind in the European Atlantic, Renewable and Sustainable Energy Reviews 154 (2022) 111889. doi:10.1016/j.rser.2021.111889.
[33] A. Martinez, G. Iglesias, Multi-parameter analysis and mapping of the levelised cost of energy from floating offshore wind in the Mediterranean Sea, Energy Conversion and Management 243 (2021) 114416. doi:10.1016/j.enconman.2021.114416.
[34] P. Beiter, W. Musial, L. Kilcher, M. Maness, A. Smith, An Assessment of the Economic Potential of Offshore Wind in the United States from 2015 to 2030, Technical Report, National Renewable Energy Laboratory (NREL), Golden, CO (United States), 2017. doi:10.2172/1349721.
[35] H. Díaz, C. Guedes Soares, An integrated GIS approach for site selection of floating offshore wind farms in the Atlantic continental European coastline, Renewable and Sustainable Energy Reviews 134 (2020) 110328. doi:10.1016/j.rser.2020.110328.
[36] E. Tercan, S. Tapkın, D. Latinopoulos, M. A. Dereli, A. Tsiropoulos, M. F. Ak, A GIS-based multi-criteria model for offshore wind energy power plants site selection in both sides of the Aegean Sea, Environmental Monitoring and Assessment 192 (2020) 652. doi:10.1007/s10661-020-08603-9.
[37] M.-A. Dupré la Tour, Photovoltaic and wind energy potential in Europe – A systematic review, Renewable and Sustainable Energy Reviews 179 (2023) 113189. doi:10.1016/j.rser.2023.113189.
[38] D. G. Caglayan, D. S. Ryberg, H. Heinrichs, J. Linßen, D. Stolten, M. Robinius, The techno-economic potential of offshore wind energy with optimized future turbine designs in Europe, Applied Energy 255 (2019) 113794. doi:10.1016/j.apenergy.2019.113794.
[39] G. Hundleby, K. Freeman, Unleashing Europe's offshore wind potential: A new resource assessment, Technical Report, Wind Europe, 2017.
[40] C. Guedes Soares, A. R. Bento, M. Gonçalves, D. Silva, P. Martinho, Numerical evaluation of the wave energy resource along the Atlantic European coast, Computers & Geosciences 71 (2014) 37–49. doi:10.1016/j.cageo.2014.03.008.
[41] G. Calado, R. Castro, Hydrogen Production from Offshore Wind Parks: Current Situation and Future Perspectives, Applied Sciences 11 (2021) 5561. doi:10.3390/app11125561.
[42] O. S. Ibrahim, A. Singlitico, R. Proskovics, S. McDonagh, C. Desmond, J. D. Murphy, Dedicated large-scale floating offshore wind to hydrogen: Assessing design variables in proposed typologies, Renewable and Sustainable Energy Reviews 160 (2022) 112310. doi:10.1016/j.rser.2022.112310.
[43] Z. Luo, X. Wang, H. Wen, A. Pei, Hydrogen production from offshore wind power in South China, International Journal of Hydrogen Energy 47 (2022) 24558–24568. doi:10.1016/j.ijhydene.2022.03.162.
[44] A. Singlitico, J. Østergaard, S. Chatzivasileiadis, Onshore, offshore or in-turbine electrolysis? Techno-economic overview of alternative integration designs for green hydrogen production into Offshore Wind Power Hubs, Renewable and Sustainable Energy Transition 1 (2021) 100005. doi:10.1016/j.rset.2021.100005.
[45] A. Lüth, P. E. Seifert, R. Egging-Bratseth, J. Weibezahn, How to connect energy islands: Trade-offs between hydrogen and electricity infrastructure, Applied Energy 341 (2023) 121045. doi:10.1016/j.apenergy.2023.121045.
[46] T. R. Lucas, A. F. Ferreira, R. Santos Pereira, M. Alves, Hydrogen production from the WindFloat Atlantic offshore wind farm: A techno-economic analysis, Applied Energy 310 (2022) 118481. doi:10.1016/j.apenergy.2021.118481.
[47] A. Giampieri, J. Ling-Chin, A. P. Roskilly, Techno-economic assessment of offshore wind-to-hydrogen scenarios: A UK case study, International Journal of Hydrogen Energy (2023). doi:10.1016/j.ijhydene.2023.01.346.
[48] B. Miao, L. Giordano, S. H. Chan, Long-distance renewable hydrogen transmission via cables and pipelines, International Journal of Hydrogen Energy 46 (2021) 18699–18718. doi:10.1016/j.ijhydene.2021.03.067.
[49] R. d'Amore Domenech, T. J. Leo, B. G. Pollet, Bulk power transmission at sea: Life cycle cost comparison of electricity and hydrogen as energy vectors, Applied Energy 288 (2021) 116625. doi:10.1016/j.apenergy.2021.116625.
[50] A. Komorowska, P. Benalcazar, J. Kamiński, Evaluating the competitiveness and uncertainty of offshore wind-to-hydrogen production: A case study of Poland, International Journal of Hydrogen Energy 48 (2023) 14577–14590. doi:10.1016/j.ijhydene.2023.01.015.
[51] Q. V. Dinh, V. N. Dinh, H. Mosadeghi, P. H. Todesco Pereira, P. G. Leahy, A geospatial method for estimating the levelised cost of hydrogen production from offshore wind, International Journal of Hydrogen Energy 48 (2023) 15000–15013. doi:10.1016/j.ijhydene.2023.01.016.
[52] A. Serna, F. Tadeo, Offshore hydrogen production from wave energy, International Journal of Hydrogen Energy 39 (2014) 1549–1557. doi:10.1016/j.ijhydene.2013.04.113.
[53] A. Babarit, F. Gorintin, P. de Belizal, A. Neau, G. Bordogna, J.-C. Gilloteaux, Exploitation of the far-offshore wind energy resource by fleets of energy ships – Part 2: Updated ship design and cost of energy estimate, Wind Energy Science 6 (2021) 1191–1204. doi:10.5194/wes-6-1191-2021.
[54] J. Bosch, I. Staffell, A. D. Hawkes, Global levelised cost of electricity from offshore wind, Energy 189 (2019) 116357. doi:10.1016/j.energy.2019.116357.
[55] RTE, 11 - L'analyse économique, in: Futurs énergétiques 2050, 2021, pp. 533–645. URL: https://assets.rte-france.com/prod/public/2022-06/FE2050%20_Rapport%20complet_11.pdf.
[56] Danish Energy Agency, Technology Data for Energy Carrier Generation and Conversion, 2017. URL: https://ens.dk/en/our-services/projections-and-models/technology-data/technology-data-renewable-fuels.
[57] BVG Associates, Guide to an offshore wind farm, Technical Report, The Crown Estate, Catapult, 2019. URL: https://www.thecrownestate.co.uk/media/2861/guide-to-offshore-wind-farm-2019.pdf.
[58] V. Timmers, A. Egea-Àlvarez, A. Gkountaras, R. Li, L. Xu, All-DC offshore wind farms: When are they more cost-effective than AC designs?, IET Renewable Power Generation (2022). doi:10.1049/rpg2.12550.
[59] National Grid ESO, Electricity Ten years statement - Appendix E Technology, Technical Report, NationalGridESO, 2013. URL: https://www.nationalgrideso.com/document/46916/download.
[60] W. Breunis, Hydrogen gas production from offshore wind energy: A cost-benefit analysis of optionality through grid connection, Ph.D. thesis, Delft University of Technology, 2021.

[61] R. d'Amore Domenech, T. J. Leo, Sustainable Hydrogen Production from Offshore Marine Renewable Farms: Techno-Energetic Insight on Seawater Electrolysis Technologies, ACS Sustainable Chemistry & Engineering 7 (2019) 8006–8022. doi:10.1021/acssuschemeng.8b06779.

[62] A. H. Reksten, M. S. Thomassen, S. Møller-Holst, K. Sundseth, Projecting the future cost of PEM and alkaline water electrolysers; a CAPEX model including electrolyser plant size and technology development, International Journal of Hydrogen Energy 47 (2022) 38106–38113. doi:10.1016/j.ijhydene.2022.08.306.

[63] M. Newborough, G. Cooley, Green hydrogen: water use implications and opportunities, Fuel Cells Bulletin 2021 (2021) 12–15. doi:https://doi.org/10.1016/S1464-2859(21)00658-1.

[64] J. Kim, K. Park, D. R. Yang, S. Hong, A comprehensive review of energy consumption of seawater reverse osmosis desalination plants, Applied Energy 254 (2019) 113652. doi:10.1016/j.apenergy.2019.113652.

[65] M. Lerch, M. De-Prada-Gil, C. Molins, A metaheuristic optimization model for the inter-array layout planning of floating offshore wind farms, International Journal of Electrical Power & Energy Systems 131 (2021) 107128. doi:10.1016/j.ijepes.2021.107128.

[66] A. Collin, A. Nambiar, D. Bould, B. Whitby, M. Moonem, B. Schenkman, S. Atcitty, P. Chainho, A. Kiprakis, Electrical Components for Marine Renewable Energy Arrays: A Techno-Economic Review, Energies 10 (2017) 1973. doi:10.3390/en10121973.

[67] P. Djapic, G. Strbac, Cost benefit methodology for optimal design of offshore transmission systems , Technical Report, Centre for Sustainable Electricity and Distributed Generation, 2008. URL: https://docplayer.net/19438524-Cost-benefit-methodology-for-optimal-design-of-offshore-transmission-systems.html.

[68] J. L. Domínguez-García, D. J. Rogers, C. E. Ugalde-Loo, J. Liang, O. Gomis-Bellmunt, Effect of non-standard operating frequencies on the economic cost of offshore AC networks, Renewable Energy 44 (2012) 267–280. doi:10.1016/j.renene.2012.01.093.

[69] M. Ikhennicheu, M. Lynch, S. Doole, F. Borsiade, F. Wendt, M.-A. Schwarzkopf, D. Matha, R. Durán Vicente, T. Habekost, L. Ramirez, S. Potestio, D3.1 Review of the state of the art of dynamic cable system design, Technical Report, INNOSEA, 2020. URL: https://corewind.eu/wp-content/uploads/files/publications/COREWIND-D3.1-Review-of-the-state-of-the-art-of-dynamic-cable-system-design.pdf.

[70] J. I. Rapha, J. L. Domínguez, Suspended cable model for layout optimisation purposes in floating offshore wind farms, Journal of Physics: Conference Series 2018 (2021) 012033. doi:10.1088/1742-6596/2018/1/012033.

[71] R. Weerheim, Development of dynamic power cables for commercial floating wind farms, Technical Report, TU Delft, 2018. URL: http://resolver.tudelft.nl/uuid:487ba1e5-2764-4e96-808c-a9ee2772219d.

[72] Y. Bai, Q. Bai, Subsea Cost Estimation, in: Subsea Engineering Handbook, Elsevier, 2010, pp. 159–192. doi:10.1016/B978-1-85617-689-7.10006-8.

[73] B. Tranberg, K. K. Kratmann, J. Stege, Determining offshore wind installation times using machine learning and open data (2019).

[74] L. Castro Santos, S. Ferreño González, V. Diaz Casas, Methodology to calculate mooring and anchoring costs of floating offshore wind devices, Renewable Energy and Power Quality Journal (2013) 268–272. doi:10.24084/repqj11.276.

[75] S. Jalili, A. Maheri, A. Ivanovic, Cost modelling for offshore wind farm decommissionning - Decomtools 2022, Technical Report, 2022. URL: https://northsearegion.eu/media/19936/cost-modelling_final_2022.pdf.

[76] J. Herdiyanti, Comparisons study of S-Lay and J-Lay methods for pipeline installation in ultra deep water, Ph.D. thesis, University of Stavanger, 2013. URL: https://core.ac.uk/download/pdf/30921158.pdf.

[77] Y. Rahmat M., Pipe-laying Method in Offshore / Subsea Construction, 2022. URL: https://indonesiare.co.id/id/article/pipe-laying-method-in-offshore-subsea-construction.

[78] Europacable, An introduction to high voltage direct current (HVDC) subsea cables systems, Technical Report, Europacable, 2012. URL: https://europacable.eu/wp-content/uploads/2021/01/Introduction-to-HVDC-Subsea-Cables-16-July-2012_.pdf.

[79] T. Stehly, P. Beiter, P. Duffy, 2019 Cost of Wind Energy Review, Technical Report, National Renewable Energy Laboratory, Golden, CO, 2020. URL: https://www.nrel.gov/docs/fy21osti/78471.pdf.

[80] A. Dewan, M. Asgarpour, Reference O&M Concepts for Near and Far Offshore Wind Farms, Technical Report, ECN, 2016. URL: https://publicaties.ecn.nl/PdfFetch.aspx?nr=ECN-E--16-055.

[81] X. Turc Castellà, Operation and maintenance costs for offshore wind farm - Analysis and strategies to reduce O&M costs, Ph.D. thesis, Universitat Politècnica de Catalunya, 2020. URL: https://upcommons.upc.edu/bitstream/handle/2117/329731/master-thesis-xavier-turc-castell-.pdf.

[82] J. V. Taboada, V. Diaz-Casas, X. Yu, Reliability and Maintenance Management Analysis on OffShore Wind Turbines (OWTs), Energies 14 (2021) 7662. doi:10.3390/en14227662.

[83] D. Cevasco, S. Koukoura, A. Kolios, Reliability, availability, maintainability data review for the identification of trends in offshore wind energy applications, Renewable and Sustainable Energy Reviews 136 (2021) 110414. doi:10.1016/j.rser.2020.110414.

[84] K. Harman, R. Walker, M. Wilkinson, Availability trends observed at operational wind farms, in: European Wind Energy Conference 2008, Brussels, 2008.

[85] N. Avanessova, A. Gray, I. Lazakis, R. C. Thomson, G. Rinaldi, Analysing the effectiveness of different offshore maintenance base options for floating wind farms, Wind Energy Science 7 (2022) 887–901. doi:10.5194/wes-7-887-2022.

[86] Y. Cai, F.-M. Bréon, Wind power potential and intermittency issues in the context of climate change, Energy Conversion and Management 240 (2021) 114276. doi:10.1016/j.enconman.2021.114276.

[87] S. Brosschot, Comparing hydrogen networks and electricity grids for transporting offshore wind energy to shore in the North Sea region. A spatial network optimisation approach., Ph.D. thesis, Utrecht University, 2022. URL: https://studenttheses.uu.nl/handle/20.500.12932/43157?show=full.

[88] A. Lepikhin, V. Leschenko, N. Makhutov, Defects Assessment in Subsea Pipelines by Risk Criteria, in: Issues on Risk Analysis for Critical Infrastructure Protection, IntechOpen, 2021. doi:10.5772/intechopen.94851.

[89] V. De Stefani, P. Carr, A Model to Estimate the Failure Rates of Offshore Pipelines, in: 2010 8th International Pipeline Conference, Volume 4, ASMEDC, 2010, pp. 437–447. doi:10.1115/IPC2010-31230.

[90] EMODnet, Human Activities, 2022. URL: https://emodnet.ec.europa.eu/en/human-activities.

[91] European Commission – Eurostat/GISCO, NUTS dataset, 2021. URL: https://ec.europa.eu/eurostat/web/gisco/geodata/reference-data/administrative-units-statistical-units/nuts.
[92] EMODnet, Bathymetry, 2018. URL: https://emodnet.ec.europa.eu/en/bathymetry.
[93] Global Fishing Watch, Datasets and Code: Apparent Fishing Effort, 2019. URL: https://globalfishingwatch.org/dataset-and-code-fishing-effort/.
[94] H. Hersbach, B. Bell, P. Berrisford, G. Biavati, A. Horányi, J. Muñoz Sabater, J. Nicolas, C. Peubey, I. Rozum, D. Schepers, A. Simmons, C. Soci, D. Dee, J.-N. Thépaut, ERA5 hourly data on single levels from 1940 to present, 2023. doi:10.24381/cds.adbb2d47.
[95] UNEP-WCMC, IUCN, Protected Planet: The World Database on Protected Areas (WDPA), 2023. URL: https://www.protectedplanet.net/en/thematic-areas/wdpa?tab=WDPA.
[96] Maritime Safety Office, World Port Index, 2019. URL: https://msi.nga.mil/Publications/WPI.
[97] G. Gualtieri, Reliability of ERA5 Reanalysis Data for Wind Resource Assessment: A Comparison against Tall Towers, Energies 14 (2021) 4169. doi:10.3390/en14144169.
[98] R. Borrmann, K. Rehfeldt, A.-K. Wallash, S. Lüers, Capacity densities of european offshore wind farms, Technical Report, Deutsche Windguard, 2018. URL: https://vasab.org/wp-content/uploads/2018/06/BalticLINes_CapacityDensityStudy_June2018-1.pdf.
[99] B. Bulder, E. Bot, G. Bedon, Optimal wind farm power density analysis for future offshore wind farms, 2018. URL: https://www.humsterlandenergie.nl/resources/LInks-duurzaam/Linkpagina/Optimal-wind-farm-power-density-analysis-for-future-offshore-wind-farms.pdf.
[100] IRENA, Green Hydrogen Cost Reduction: Scaling up Electrolysers to Meet the 1.5°C Climate Goal, Technical Report, International Renewable Energy Agency, Abu Dhabi, 2020. URL: https://www.irena.org/publications/2020/Dec/Green-hydrogen-cost-reduction.
[101] European Commission, A Clean Planet for All, 2018.
[102] A. Rogeau, R. Girard, M. De Coatpont, J. Vieubled, G. Erbs, P. Affonso Nobrega, Techno-economic evaluation and resource assessment of hydrogen production through offshore wind farms: a European perspective - Supplementary material, 2023. doi:https://doi.org/10.5281/zenodo.8036703.
[103] K. Donkers, Hydrogen production on offshore platforms - A techno-economic analysis, Ph.D. thesis, Utrecht University, 2020. URL: https://studenttheses.uu.nl/bitstream/handle/20.500.12932/37491/Thesis%20research%20Koen%20Donkers%20-%20%20Final%20version.pdf?sequence=1.
[104] J. Braga, T. Santos, M. Shadman, C. Silva, L. F. Assis Tavares, S. Estefen, Converting Offshore Oil and Gas Infrastructures into Renewable Energy Generation Plants: An Economic and Technical Analysis of the Decommissioning Delay in the Brazilian Case, Sustainability 14 (2022) 13783. doi:10.3390/su142113783.
[105] ACER, Transporting pure hydrogen by repurposing existing gas infrastructure: overview of existing studies and reflections on the conditions for repurposing, Technical Report, European Union Agency for the Cooperation of Energy Regulators, 2021. URL: https://acer.europa.eu/Official_documents/Acts_of_the_Agency/Publication/Transporting%20Pure%20Hydrogen%20by%20Repurposing%20Existing%20Gas%20Infrastructure_Overview%20of%20studies.pdf.
[106] G. Cauchois, C. Renaud-Bezot, M. Simon, V. Gentile, M. Carpenter, L. Even Torbergsen, Re-Stream - Study on the reuse of oil and gas infrastructure for hydrogen and CCS in Europe, Technical Report, Carbon Limits, 2021. URL: https://www.concawe.eu/wp-content/uploads/Re-stream-final-report_Oct2021.pdf.